INVESTIGATION OF THE BENEFITS OF VARIABLE ORIFICE DAMPERS USED IN AN EARTHQUAKE EXCITED THREE STORY STRUCTURE

A Thesis Submitted to
The Graduate School of Engineering and Sciences of
İzmir Institute of Technology
in Partial Fulfillment of the Requirements for the Degree of

MASTER OF SCIENCE

in Civil Engineering

by
Hakan GÖKDAĞ

November 2009

İZMİR

We approve the thesis of **Hakan GÖKDAĞ**

Assist. Prof. Dr. Gürsoy TURAN
Supervisor

Assist. Prof. Dr. Ersin AYDIN
Committee Member

Assoc. Prof. Dr. Serhan ÖZDEMİR
Committee Member

09 November 2009

Prof. Dr. Gökmen TAYFUR
Head of the Civil Engineering Department

Assoc. Prof. Dr. Talat YALÇIN
Dean of the Graduate School of
Engineering and Sciences

ACKNOWLEDGEMENTS

I am very grateful for the encouragement, guidance, understanding, and support of my advisor, Assst. Prof. Dr. Gürsoy TURAN, for keeping me focused in my research throughout this study.

I also would like to thank Assst. Prof. Dr. Serhan ÖZDEMİR and Assst. Prof. Dr. Ersin AYDIN for their valuable helps and advises.

Thanks to the many people at IYTE Department of Civil Engineering who helped me in anyway in this study.

This study would not be possible without the support of The Scientific and Technical Research Council of Turkey (TUBİTAK Project number 107M353).

Many thanks to my colleagues Timur ÖZDEMİR, Başak DOĞAN, Doruk YORMAZ and Fırat PULAT for having good times during coffee breaks.

Finally, I would like to thank my mother and father for their boundless love and for all they have done for me.

ABSTRACT

INVESTIGATION OF THE BENEFITS OF VARIABLE ORIFICE DAMPERS USED IN AN EARTHQUAKE EXCITED THREE STORY STRUCTURE

Research in the field of control of civil engineering structures is a continuing process. The three basic approaches to structural control may be defined as follows passive control systems,active control systems and semi-active control systems. These systems have received much attention recently because they have versatility and adaptability of active control systems. Although there is a wide variety of these energy absorbing devices, but all have one thing in common – they absorb energy from the structure. Semi-active control systems possess the advantages of both active and passive control systems. Variable orifice dampers are semi-active control devices that utilize the hydraulic fluid flow to generate controllable damping forces. Depending on the state of the structure, the energy absorbing property of the variable orifice dampers is changed on the fly. In this study, the proposed semi-active control algorithm and the effect of variable orifice damper for seismic response reduction is examined. To demonstrate the efficiency of the proposed semi-active control algorithm and the usefulness of variable orifice dampers,controlled and uncontrolled behaviour of the three story model structure subjected to earthquake forces are investigated numerically. The three story model structure in Civil Engineering Laboratory in İYTE is utilized for numerical simulations. The results indicate numerically that the proposed semi-active control algorithm with a variable orifice damper can be used effectively to reduce the earthquake induced structural vibrations.

ÖZET

DEGİŞKEN SÖNÜMLEMELİ AMORTİSÖRLERİN DEPREM ETKİSİ ALTINDAKİ ÜÇ KATLI BİR YAPIYA OLAN FAYDASININ DEĞERLENDİRİLMESİ

Günümüzde inşaat mühendisliği yapılarının kontrolü üzerine yoğun çalışmalar devam etmektedir. Üç temel yapı kontrol yaklaşımı şu şekilde pasif, aktif ve yarı-aktif kontrol sistemleri olarak sıralanabilir. Bu sistemler son yıllarda çok dikkat çekmiştir çünkü bu sistemler çok yönlülük ve adaptasyon özelliklerine sahiptirler. Bu sistemler arasında çok çeşitlilik olmasına rağmen, ilkede hepsi aynı amacı güder – sistemden enerji emmek. Yarı-aktif kontrol sistemleri pasif ve aktif kontrol sistemlerinin avantajlarına sahiptirler. Değişken katsayılı amortisörler yarı aktif kontrol aygıtlarıdır ve hidrolik sıvı akışından faydalanarak kontrollü sönümleme kuvveti üretirler. Aygıtın sönümleme katsayısı yapının durumuna (deformasyonu ve deformasyon hızı) göre değiştirilebilir. Depremin etkisini azaltmak için önerilen method ve değişken katsayılı amortisörün etkisi bu çalışmada irdelenmiştir. Önerilen methodun verimliliğini ve değişken katsayılı amortisörlerin faydasını göstebilmek için deprem kuvvetleri etkisi altındaki üç katlı model yapının kontrollü ve kontrolsüz davranışı sayısal olarak incelenmiştir. İYTE inşaat mühendisliği yapı laboratuarında bulunan üç katlı model yapı sayısal simulasyonlar için kullanılmıştır. Bu çalışmada elde edilen sonuçlar önerilen yarı aktif kontrolün depremin neden olduğu yapısal titreşimleri azalmada efektif olarak kullanılabileceğini sayısal olarak göstermiştir.

TABLE OF CONTENTS

LIST OF FIGURES

Figure **Page**

LIST OF TABLES

CHAPTER 1

INTRODUCTION

1.1.Overwiew

In the last three decades, many earthquakes with strong magnitude have been observed all over the world. In this respect, future earthquakes may cause billions of dollars of damage, and major loss. Therefore, in the recent years, civil engineers tried to find out new methods to reduce the effects of earthquakes and to improve the response of structures subjected to external excitation. With the light of this perspective, a new and remarkable idea has attracted increasing attention in many areas of civil engineering application .This view is based on idea that the response of structures can be enhanced by the use of structural control technologies. There are mainly three control approaches that can be classified as either passive, active or semi-active. A passive control application is a system, which produces a control force by using the motion of the structure and does not need an external power source (see Figure 1-1-a). Active control systems need a considerable amount of external energy to power actuators that provide the necessary control force to the structure (see Figure 1-1-b). The principles of semi-active control systems are based on the idea that the response of the structures can be reduced by using passive control devices (for example: dampers). The control consists of changing the physical parameters of the devices . Semi-active control systems do not require a large power source.

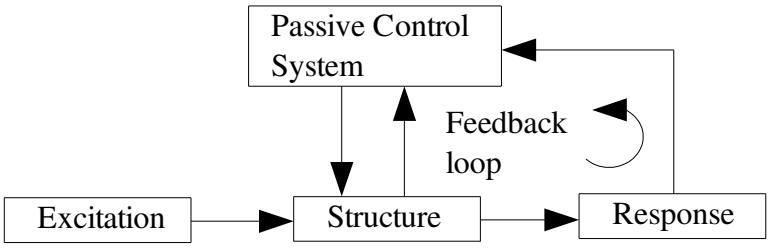

(a)

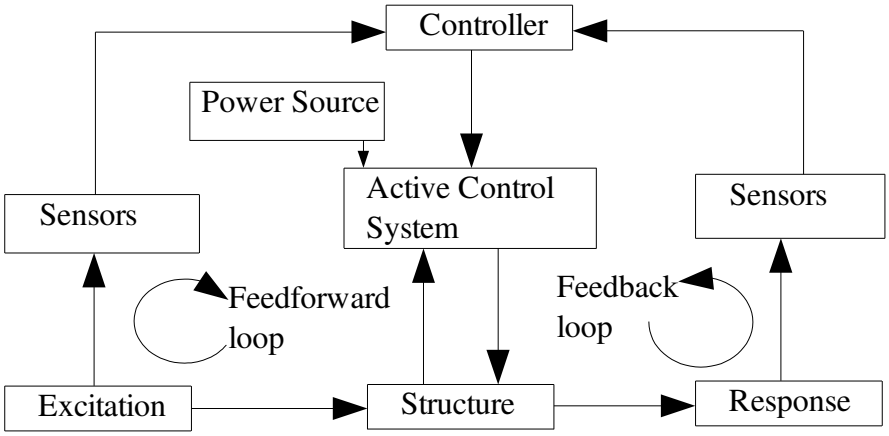

(b)

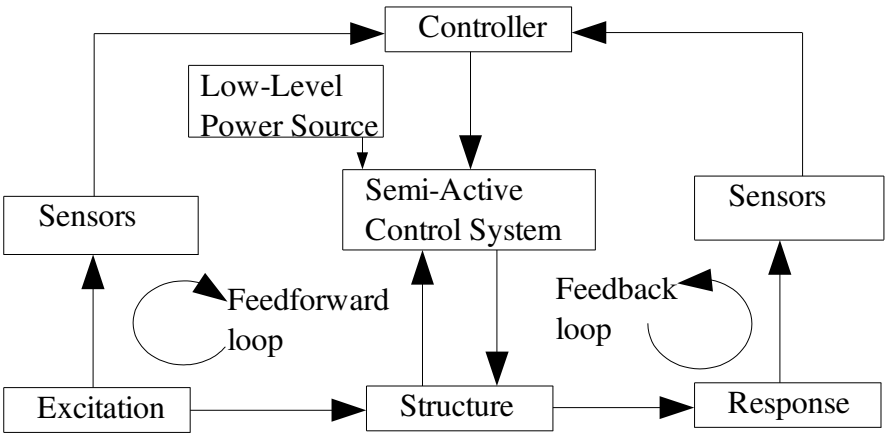

(c)

Fig. 1.1 Block diagrams of structural control systems: (a) passive control system, (b) active control system and (c) semi-active control system

Over the last three decades, there has been much development and diversity of control devices to protect structures from dynamic loads. Control devices provide a reduction in the building's response to seismic activity. There are several types of passive control devices such as base isolation, tuned mass dampers, and supplemental dampers. With that in mind, the development and experimental testing of semi-active control systems and devices have been investigated in the recent past. Semi-active control devices are designed such that their physical properties can be changed during an external excitation. Most investigators seek to enhance control algorithms for these devices, including a clipped optimal control algorithm (Sack 1994), a bang-bang algorithm (Patten,et al. 1994), a Linear Quadratic Regulator (LQR) algorithm (Symans and Constantinou1995, Sadek and Mohraz 1998), a Sliding Mode Control (SMC) algorithm (Symans and Constantinou 1995, Yang, et al. 1995), a generalized LQR algorithm with a penalty on the acceleration response (Sadek and Mohraz 1998), and a displacement-acceleration domain algorithm (Sadek and Mohraz 2003.) The first full-scale application of structural control in the United States, shown in Figure 1-3, consisted in the installation of such devices on a bridge on Interstate 35, near Purcell, Oklahoma (1999). Variable-orifice dampers have also been applied to buildings. Kurata et al. (1999;2000), for example, describe the implementation of eight variable-orifice dampers in a five-story building in Shizuoka City, Japan.

Fig.1.2. Full-Scale Experiment on Interstate 35 in Oklahoma

Semi-active control systems have recently been applied to civil engineering structures. A semi-active control system generally originates from a passive control system which has been subsequently modified to allow for adjustment of mechanical properties (Symans and Constantinou 1995). Semi-active control systems are separated into two groups; active variable stiffness and active variable damping. In the first group, the stiffness of the structure is varied to reduce the structural response. In the second group, semi-active control devices allow adjustments in their mechanical properties to achieve reductions in the structural response.

One of the challenges in the application of control systems to civil structures is the placement of control devices. However, typical placement of the control devices to civil structures are performed for a long time. Figure 1-3-a and Figure 1-3-b show the typical placements of the control devices to civil structures. In the first type, control device is installed between the ground and the first floor as shown in Figure 1-3-b. This type of location can be easily located to civil structures. In the second type, control devices are placed in the each floor to modify its responses as shown in Figure 1- 3-a. As would be expected, this type of placement is more efficient than the other application, since more control devices are present.

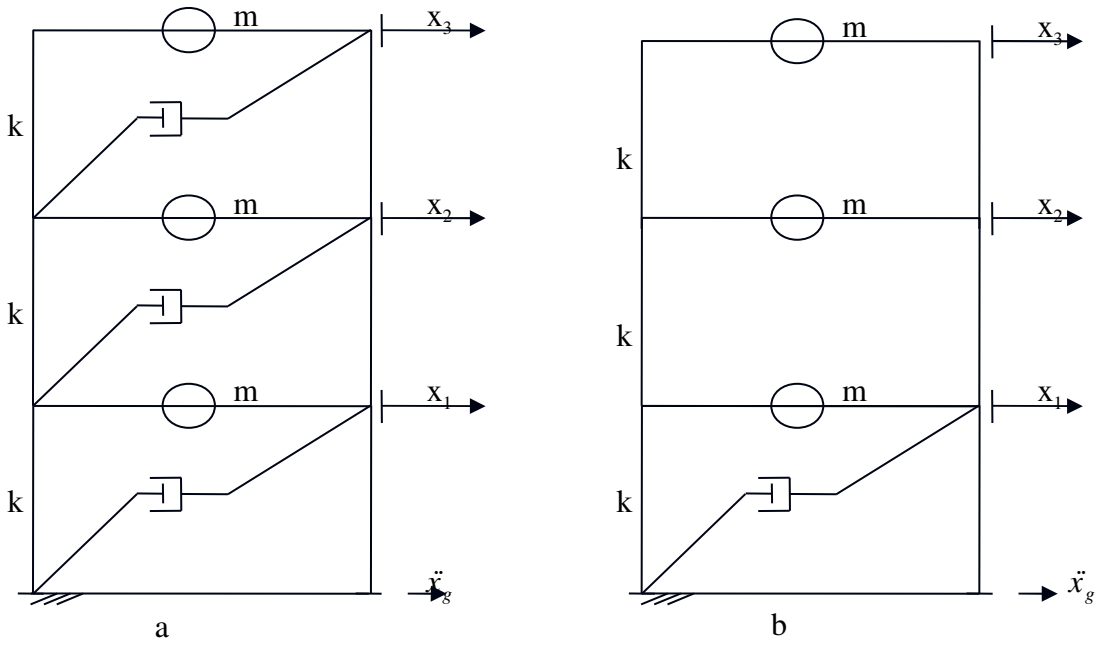

Figure 1.3. Control Device Placement

Symans and Constantinou (1995) have studied a semi-active fluid damper, which consists of a stainless steel piston rod, a bronze piston head, a piston rod make-up accumulator and the damper is filled with a thin silicone oil (see Figure 1-4). The damping force is developed as the result of a pressure differential across the piston head. The orifices in the piston head are specified to enable a minimum fluid flow, which is necessary to hinder an infinite damping force when the control valve is completely closed. This damper design results in a force output that depends on the adjustment of the control valve. Results indicate that semi-active control with variable damper may be efficient in reducing the response.

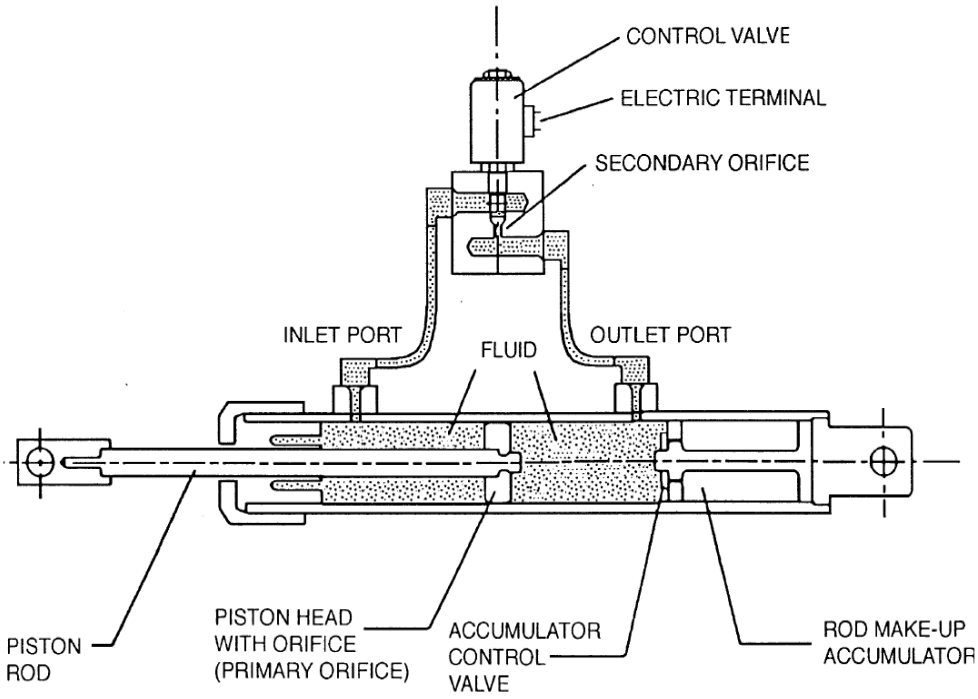

Figure 1.4. Construction of tested semi-active fluid damper

1.2. Equations of Motions

The equation of motion for a building with control forces and disturbance forces is given as follows, in which the structure is idealized as a shear-type building.

$$[M]\ddot{u}+[C]\dot{u}+[K]u=\Gamma f-[M]\Lambda\ddot{u}_g \tag{1.1}$$

where [M] is the mass matrix, [C] is the damping matrix of the bare frame structure, [K] is the stiffness matrix, {f} is the control force vector , { Γ }is a vector of ones and zeros describing the placement of the control force in the structure, { Λ } is a vector of ones, $\ddot{u}_g$ is the ground acceleration, and { $\ddot{u}$ }, { $\dot{u}$ }, and {u} are the relative acceleration, velocity, and displacement vectors, respectively.

1.3. Model Building ; Case Study

Figure 1-5 is a picture of the semi-actively controlled, three-story, model building at the Structural Dynamics and Control/Earthquake Engineering Laboratory at the İzmir Institute of Technology. The test structure used in this numerical study is designed to be a scale model with the same frequencies of a general type building and is subjected to a one-dimensional ground motion.

Figure 1.5. Model Building

The model steel building frame has a height of 270 cm. The structure is selected to have a mass of 100 kg at each floor. Modal damping is assumed and the damping ratio of each mode in the uncontrolled structure is 2%. The structure was designed to have equal stiffness on each floor with a fundamental natural frequency at 2.0 Hz.

CHAPTER 2

MODELLING THE BUILDING

2.1. Introduction

A three-story model building is used to perform numerical studies on the behavior of the semi-active control systems. The structure was modeled as a shear mass building. The structure is subjected to earthquake ground motion in one direction, only. This corresponds to the weak direction of the building model, whereas no deformation is expected in the perpendicular direction, since its stiffness is 100 times larger. The total mass of the three-story structure was 600 kg, each floor has an equal mass of 200 kg. The structure was simulated with two dampers which are installed between the ground and the first floor (see Figure 2.1)

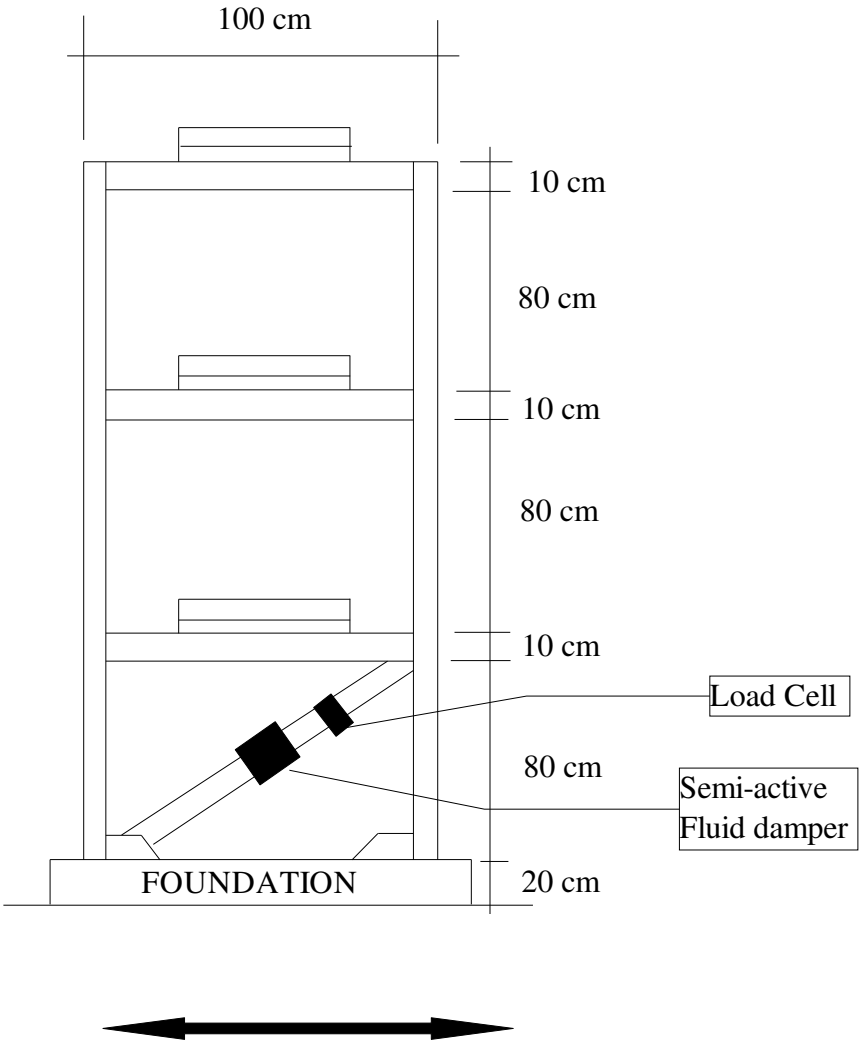

Figure 2.1.Schematic of Model Structure

2.2. Shear Building Model

In this study, a three -story model structure was idealized as a shear building model (see Figure 2.2). This idealization is based on the following assumptions.

The floors are infinite rigid and incompressible. The floors and the ground provide a fixed support to the columns. Hence, there are no floor rotations. The rigid ground implies that the ground acceleration is applied to all columns equally.

All the mass of the floor is lumped at the center of mass of the floor. The mass center of the floor coincided with the stiffness-center of the floor. (see Figure 2.2).

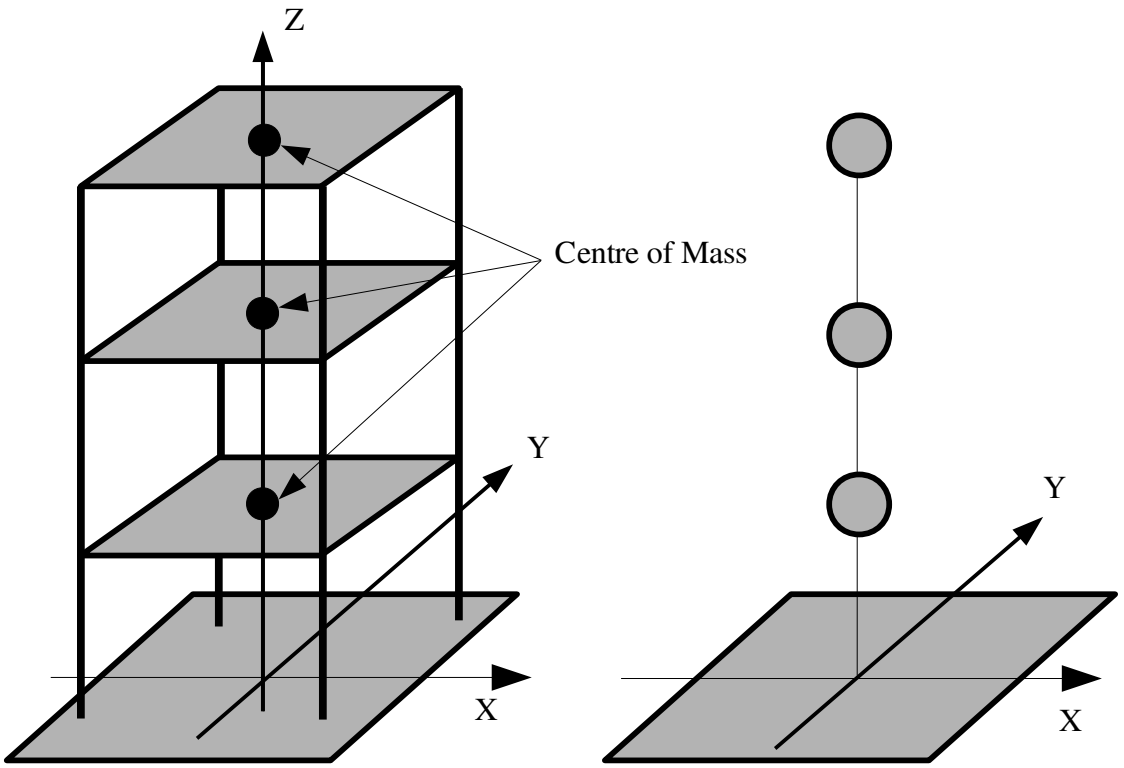

Figure 2.2 . Three-story Shear Building

2.3. Horizontal equation of motion (neglecting damping)

Consider of the idealised structure subject to ground motion in the x direction. Figure 2.3 shows the flree body diagram of a typical floor. The horizontal shear force induced by the bending of the columns above and below (the stiffness forces) must be balanced with the mass horizontal inertia force of the floor.

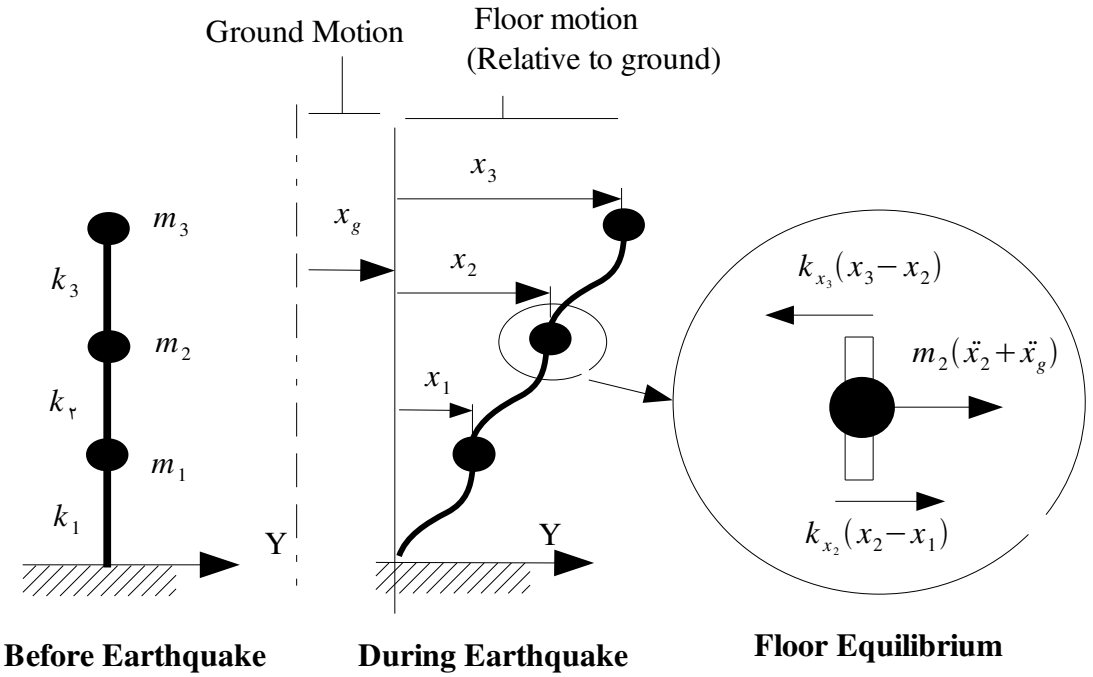

Figure 2.3 . Horizontal Motion

Hence for the second floor,

$$\underbrace{(m_2(\ddot{x}_2+\ddot{x}_g))}_{force}+\underbrace{(k_{x_2}(x_2-x_1)-k_{x_3}(x_3-x_2))}_{elastic\ force}=0 \qquad (2.1)$$

and after some manipulations

$$m_2\ddot{x}_2-k_{x_2}x_1+(k_{x_2}+k_{x_3})x_2-k_{x_3}x_3=-m_2\ddot{x}_g \qquad (2.2)$$

A similar approach is used to obtain the equation of motion for the first and the third floor.

$$m_1\ddot{x}_1+(k_{x2}+k_{x3})\,x_1-k_{x2}\,x_2=-m_1\ddot{x}_g \tag{2.3}$$

$$m_3\ddot{x}_3-k_{x_3}x_2+k_{x_3}x_3=m_3\ddot{x}_3 \tag{2.4}$$

Hence, a matrix form of equation is obtained as follows

$$M\,\ddot{x}+K_x=-M1\,\ddot{x}_g \tag{2.5}$$

The explicit matrix system is for a three-story building.

$$\mathrm{M}\begin{vmatrix}\ddot{x}_3\\ \ddot{x}_2\\ \ddot{x}_1\end{vmatrix}+\underbrace{\begin{vmatrix}k_{x3} & -k_{x3} & 0\\ -k_{x3} & k_{x2}+k_{x3} & -k_{x2}\\ 0 & -k_{x2} & k_{x1}+k_{x2}\end{vmatrix}}_{K}\begin{vmatrix}\ddot{x}_3\\ \ddot{x}_2\\ \ddot{x}_1\end{vmatrix}=\text{-M}\begin{vmatrix}1\\1\\1\end{vmatrix}\ddot{x}_g \tag{2.6}$$

$$\text{Mass matrix ,[M]=}\begin{vmatrix}m_3 & 0 & 0\\ 0 & m_2 & 0\\ 0 & 0 & m_1\end{vmatrix} \tag{2.7}$$

where m_1 , m_2 and m_3 are the mass of the first, second and third story, respectively.

$$\text{Stiffness matrix, [K]=}\begin{vmatrix}k_{x3} & -k_{x3} & 0\\ -k_{x3} & k_{x2}+k_{x3} & -k_{x2}\\ 0 & -k_{x2} & k_{x1}+k_{x2}\end{vmatrix} \tag{2.8}$$

, where k_{x1} , k_{x2} and k_{x3} are the stiffnesses of the first,second and third story, respectively.

The story stiffness is obtained with the sum of the lateral stiffness of all columns in the story. Thus the story stiffness is

$$k_{xi} = \frac{12\mathrm{EI}_{yi}}{L_i^3} n \tag{2.9}$$

where n is the number of columns for each floor. L is the length of the columns. EI_y is the flexural stiffness of a typical column bending in the x direction about the y axis (see Figure 2.4).

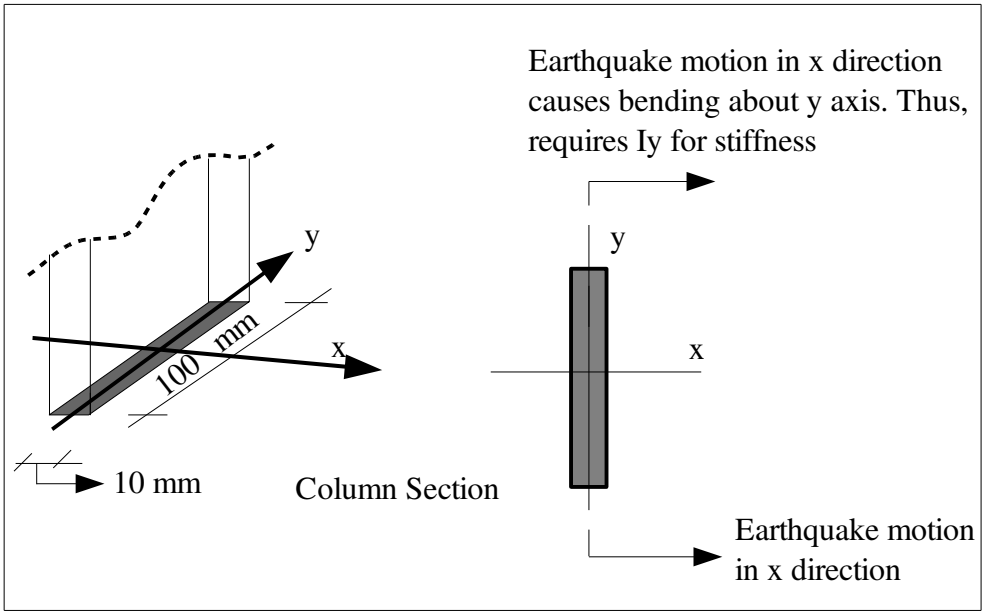

Figure 2.4 . Flexural Rigidity

$$\text{Hence,} \quad I_y = \frac{100 * 10^3}{12} = 8333.33\, mm^3 \tag{2.10}$$

$$E = 200000\, N/mm \tag{2.11}$$

$$L = 800\,mm \quad , \quad n = 4 \tag{2.12}$$

$$k_x = \frac{12\mathrm{EI}_y}{L^3} n = (\frac{12 * 200000 * 8333.33}{800^3}) * 4 = 156.25\,N/mm \tag{2.13}$$

$$I_{beam} = \frac{(90^3 - 80^3)(90 - 80)}{12} = 180833.3\,mm^4 \tag{2.14}$$

$$I_{column} = \frac{100 * 10^3}{12} = 8333.33\,mm^3 \tag{2.15}$$

$$I_{column} = \frac{100 * 10^3}{12} = 8333.33\,mm^3 \tag{2.16}$$

$$(\frac{EI}{L})_{beam} = 200000\,180833.3/1000 = 36166660\,N - mm \tag{2.17}$$

$$(\frac{EI}{L})_{column} = 200000\,8333.33/800 = 2083333.25\,N - mm \tag{2.18}$$

The beam rigidity is much bigger than column. Thus, the column ends is acceptable as a fixed supports.

In this study, all column of the three-storey building are identical in cross section and their type of end fix.

Hence,

$$k_{x1} = k_{x2} = k_{x3} = 156.25\,N/mm \tag{2.19}$$

$$m_1 = m_2 = m_3 = 0.200\,N - s^2/mm \tag{2.20}$$

Substituting these data in the stiffness matrix and mass matrix, then we can obtain,

$$\text{Mass matrix} \quad [M]=\begin{bmatrix} 0.200 & 0 & 0 \\ 0 & 0.200 & 0 \\ 0 & 0 & 0.200 \end{bmatrix}, \quad N-s^2/mm\,(ton) \tag{2.21}$$

$$\text{Stiffness Matrix} \quad [K]=\begin{bmatrix} 156.25 & -156.25 & 0 \\ -156.25 & 312.5 & -156.25 \\ 0 & -156.25 & 312.5 \end{bmatrix}, \quad N/mm \tag{2.22}$$

2.4 . Construction Damping Matrix

A simple procedure was used to determine a classical damping matrix from damping ratios.The procedure assumes linearly elastic response of the structure.

The equation of motion of the three-story structure are given by Equation1.1. Express displacement , velocity and acceleration vectors in terms of the generalized coordinates:

$$\{u(t)\}=[\Phi]\{q(t)\} \quad , \quad \{\dot{u}(t)\}=[\Phi]\{\dot{q}(t)\} \quad , \quad \{\ddot{u}\}=[\Phi]\{\ddot{q}(t)\} \tag{2.23}$$

where $[\Phi]$ is the modal vector ,q(t) is known as the generalized coordinates and define the nature of the response and the relative magnitude of the modes.

Rewrite equation of motion in terms of the generalized coordinates:

$$[M][\Phi]\{\ddot{q}\}+[C][\Phi]\{\dot{q}\}+[K][\Phi]\{q\}=-[M]\{1\}\ddot{u}_g \tag{2.24}$$

Premultiply by $[\Phi]^T$

$$[\Phi]^T[M][\Phi]\{\ddot{q}\}+[\Phi]^T[C][\Phi]\{\dot{q}\}+[\Phi]^T[K][\Phi]\{q\}=-[\Phi]^T[M]\{1\}\ddot{u}_g \tag{2.25}$$

A convenient means of normalizing the mode shapes is

$$[\Phi]^T[M][\Phi]=[I] \tag{2.26}$$

$$[\Phi]^T[K][\Phi]=\begin{bmatrix} w_1^2 & 0 & 0 \\ 0 & w_2^2 & 0 \\ 0 & 0 & 0 \\ 0 & 0 & 0 \\ 0 & 0 & w_n^2 \end{bmatrix} \tag{2.27}$$

$$c=[\Phi]^T[C][\Phi]=\begin{bmatrix} 2*\varsigma*w_1 & 0 & 0 \\ 0 & 2*\varsigma*w_2 & 0 \\ 0 & 0 & 0 \\ 0 & 0 & 0 \\ 0 & 0 & 2*\varsigma*w_n \end{bmatrix} \tag{2.28}$$

Now we can apply to determine a classical damping matrix from modal damping ratios.In order to do this,we can start to utilize :

$$c=[\Phi]^T[C][\Phi] \tag{2.29}$$

where c is a diagonal matrix which is defined tin Equation 2.28

With ς is estimated as selected in necesseary chart,c is known from and Equation 2.28 from Equation 2.29, damping matrix can be obtained as

$$C=([\Phi]^T)^{-1}[c][\Phi]^{-1} \tag{2.30}$$

As a result,we can compute the damping matrix using this Equation 2.30.

2.5. Mode Shapes of the Model Building

In order to compute the damping matrix.we should find the mode shapes of the model building with respect to Equation 2.30. Thus,the structural analysis program was developed to find mode shapes of the model building. A computer program scilab is used to write the analysis program. A summary of the dynamic properties of the three story model building is presented in Table 2.1. Figure 2.5-Figure 2.7 show the first three modes shapes of the model building.

Table 2.1 Dynamic Properties of the Three-Storey Structure

Mode		1	2	3
Frequency(Hz)		1.98	5.55	8.02
Damping ratio(%)		0.02	0.02	0.02
Mode Shapes	Floor 3	1.00	1.00	1.00
	Floor 2	0.80	-0.55	-2.25
	Floor 1	0.45	-1.25	1.80

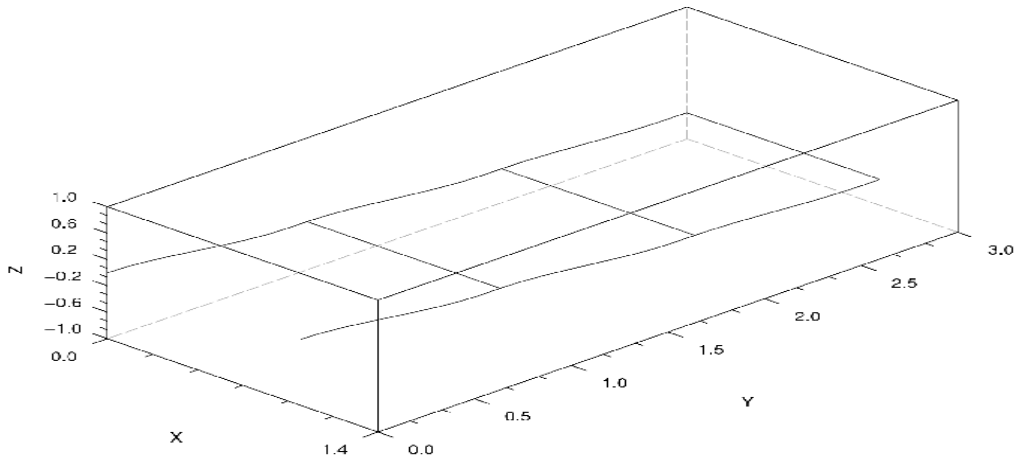

Figure 2.5 Fundamental Mode of The Model Building

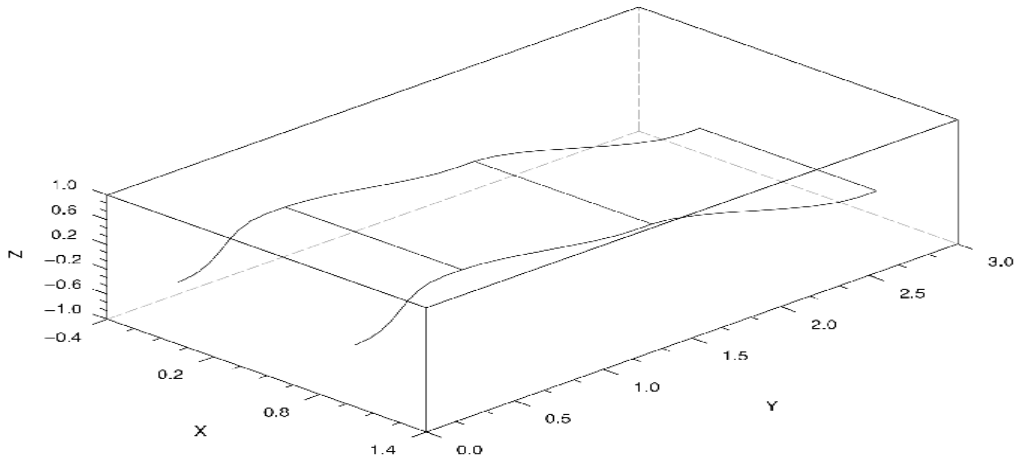

Figure 2.6. Second Mode of The Model Building

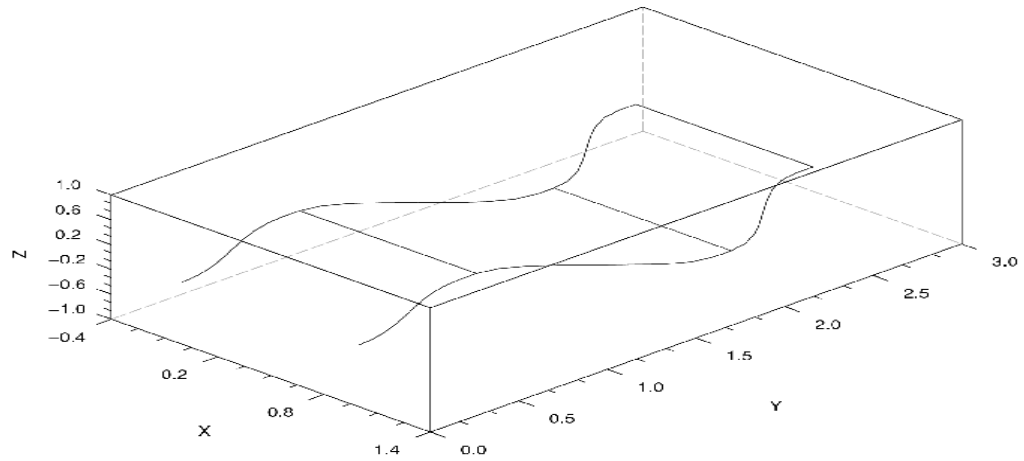

Figure 2.7. Third Mode of The Model Building

Normalized mode shapes matrix:

$$[\Phi]=\begin{vmatrix} 2.3305235 & 1.8689347 & -1.0371805 \\ 1.8689347 & -1.0371805 & 2.3305235 \\ 1.0371805 & -2.3305235 & -1.8689347 \end{vmatrix} \quad , \quad [\Phi]^T[M][\Phi]=[I] \tag{2.31}$$

Substituting the normalized mode shape matrix and c is known from Equation 2.28 in Equation 2.30 give the damping matrix:

$$[C]=\begin{vmatrix} 0.0973941 & -0.0540496 & -0.0096450 \\ -0.0540496 & 0.1417987 & -0.0444046 \\ -0.0096450 & -0.0444046 & 0.1514437 \end{vmatrix} \tag{2.32}$$

CHAPTER 3

LQR CONTROL METHOD

3.1.Introduction

The Linear Quadratic Regulator (LQR) control design and its application to the three-storey model structure with variable dampers is demonstrated in this chapter. The LQR control method is used to optimize the structural response and the amount of damper force for the three-storey model structure. In the previous chapter, the mass, damping, and stiffness matrices were created by constructing a three-storey finite element model. The sensor and variable damper model were constructed and induced to the state space model of the building to form the design model. The weighting matrices were selected to give best reduction in the response of the model building. The variable damper was inserted to the three-storey model structure and then simulated under earthquake acceleration records. Three different records were used as input to simulation of the three-storey model structure. One of them was the north-south component of the El Centro record obtained during the 1940 earthquake in the Imperial Valley. The other two motions were based on the Kocaeli-Sakarya and Düzce-Bolu earthquake records obtained from Düzce and Bolu stations.

3.2. The Reason for Using Semi-Active Control Devices

In order to examine the effect of the damper to the three story model structure, a set of simulations are carried out. In these simulations, damper coefficients are changed from 1 to 30 N-s/mm. Maximum story displacements and accelerations values for the El Centro, Düzce-Bolu and Kocaeli-Sakarya earthquake excitations are recorded for each damper coefficient and are plotted with respect to the damper coefficient (Figure 3.1-Figure 3.6). The results are also presented in Table 3.1 and Table 3.2.

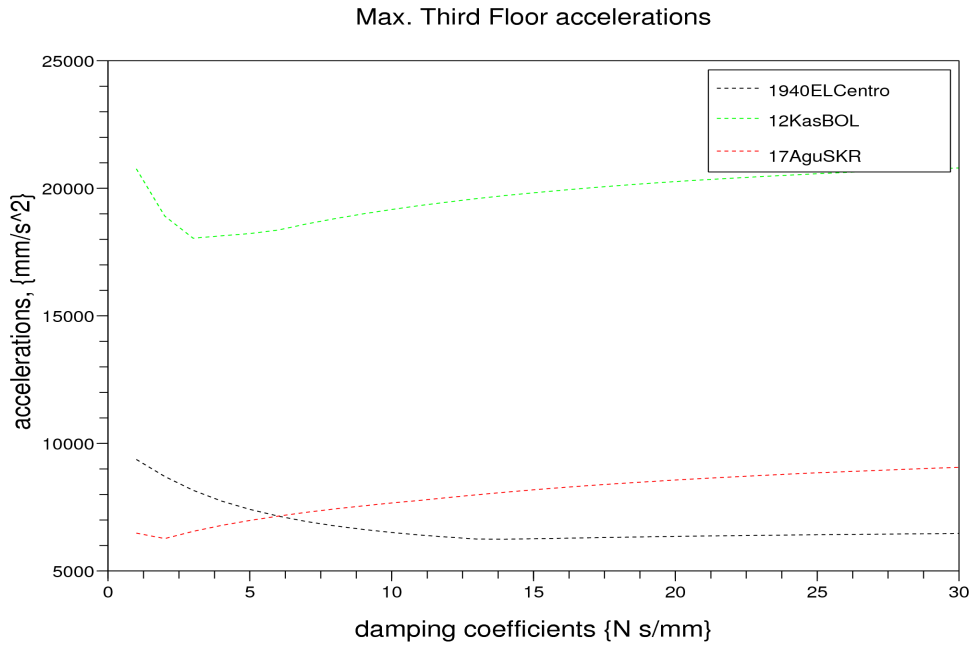

Figure 3.1. Maximum Third Floor Acceleration Values with respect to the Damper Coefficient

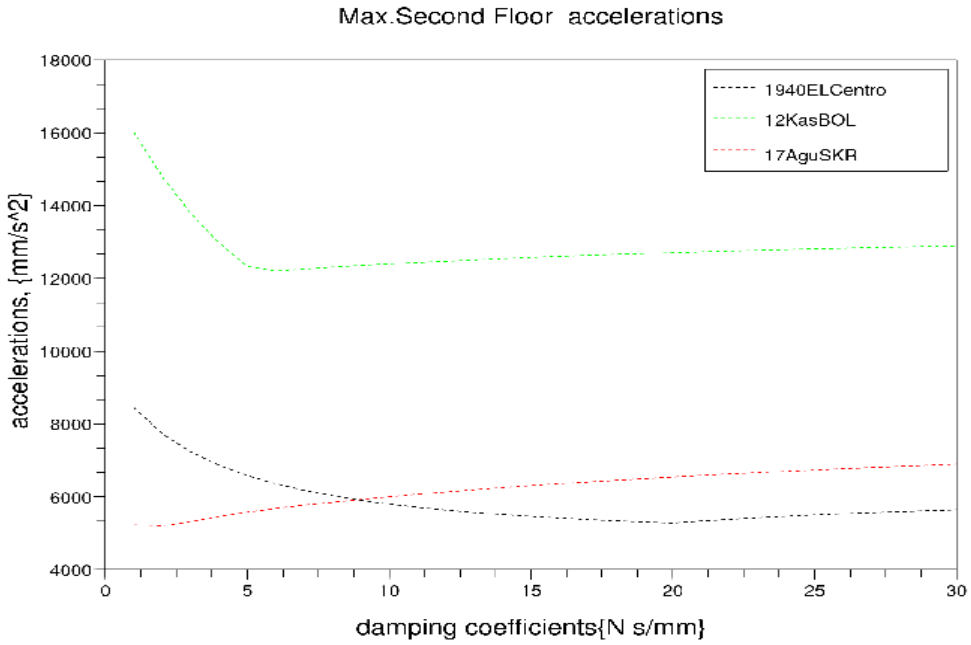

Figure 3.2. Maximum Second Floor Acceleration Values with respect to the Damper Coefficient

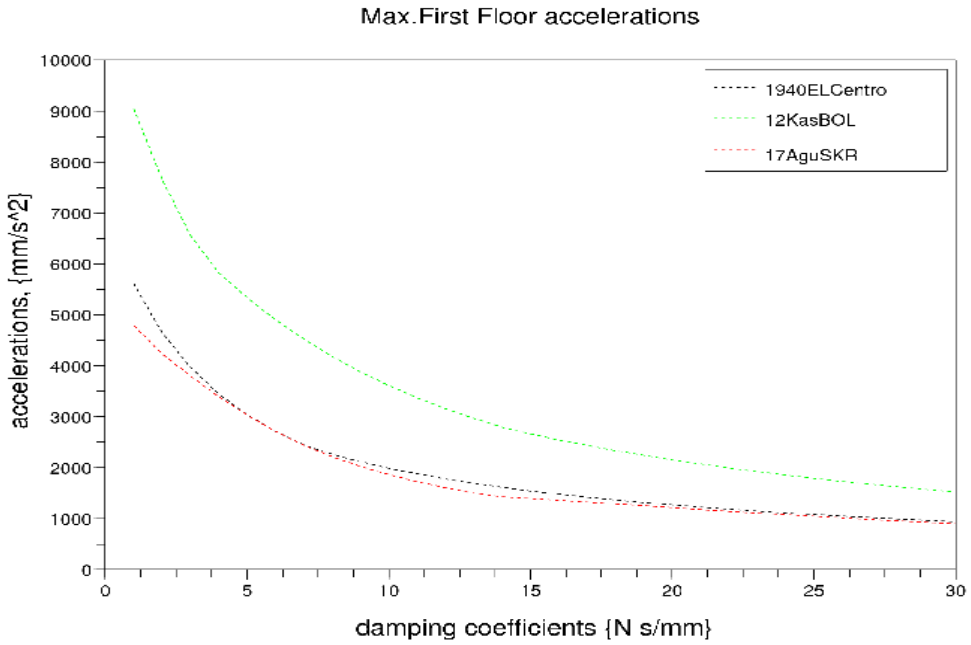

Figure 3.3. Maximum First Floor Acceleration Values and with respect to the Damper Coefficie

Table 3.1. Optimum Damper Coefficients Calculated Using Maximum Acceleration Values

Excitation	Story Number	Optimum Damper Coefficients copt, (N-sec\mm)	Corresponding max.Acceleration Values (mm\s2)
El Centro	3th	13	6250
	2th	20	5290
	1th	30	950
Düzce-Bolu	3th	3	18050
	2th	6	12210
	1th	30	1530
Kocaeli-Sakarya	3th	2	6270
	2th	2	5206
	1th	30	910

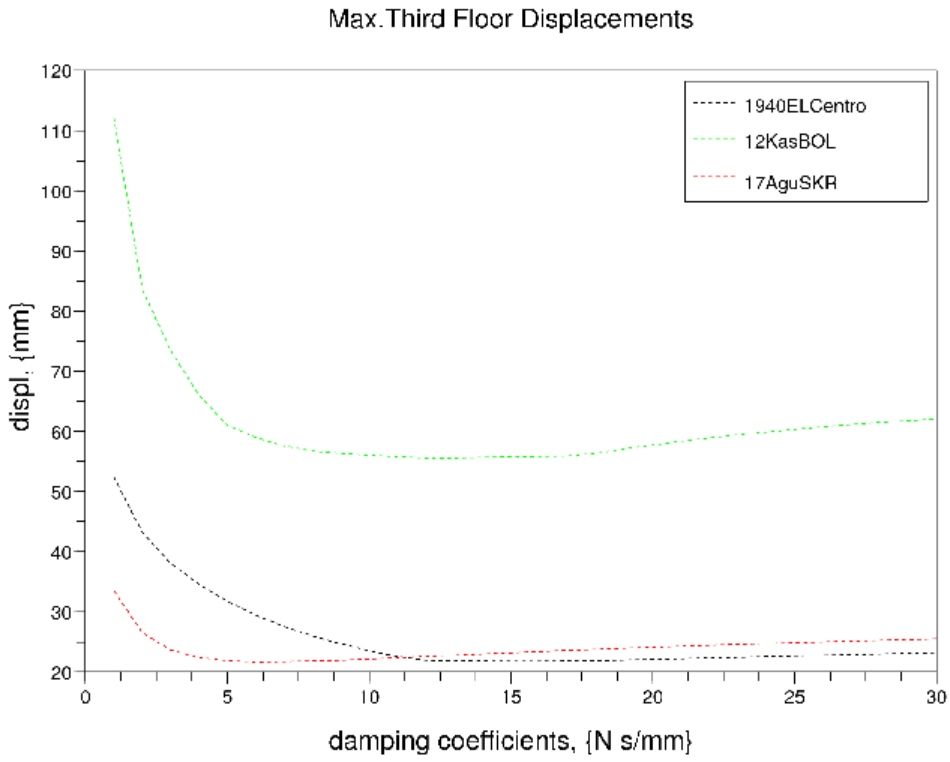

Figure 3.4. Maximum Third Floor Displacement Values and Damper Coefficients

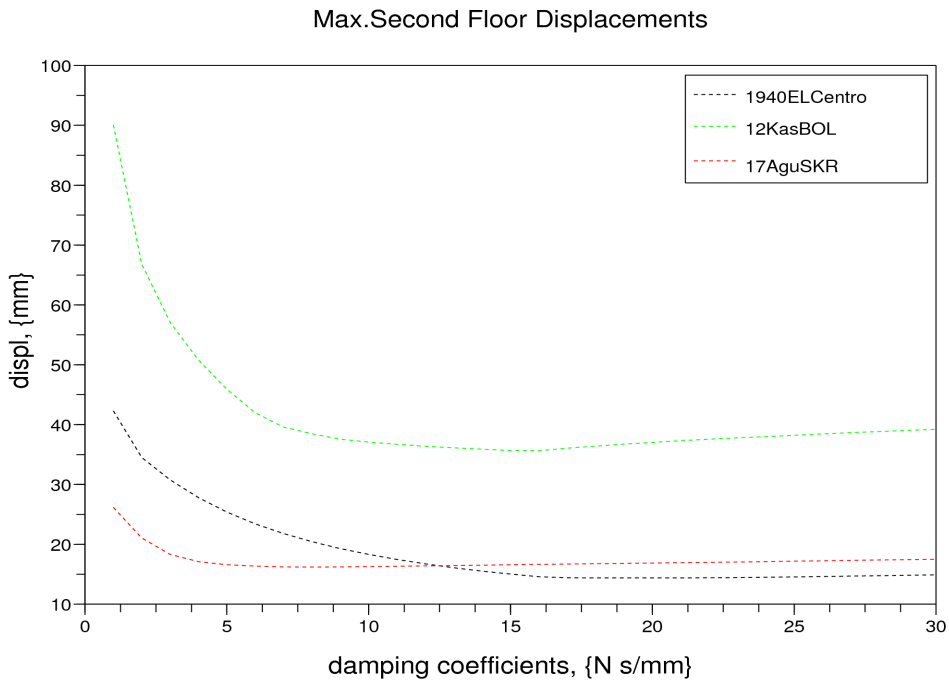

Figure 3.5. Maximum Second Floor Displacement Values and Damper Coefficients

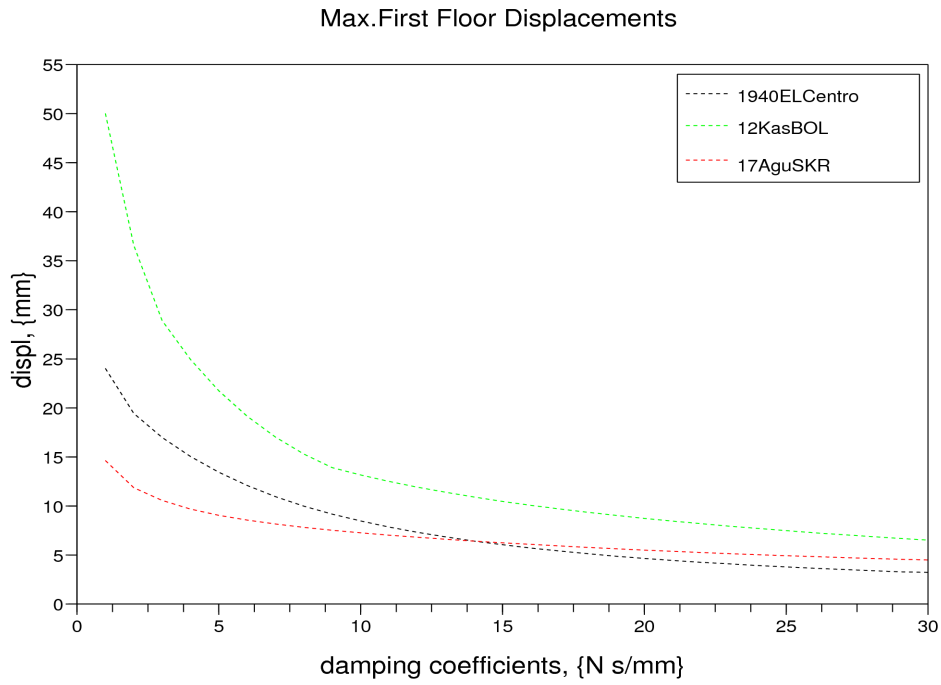

Figure 3.6. Maximum First Floor Displacement Values and Damper Coefficients

Table 3.2. Optimum Damper Coefficients Calculated Using Maximum Displacement Values

Excitation	Story Number	Optimum Damper Coefficients copt, (N-sec\mm)	Corresponding max.Displacement Values (mm)
El Centro	3th	12	21.9
	2th	18	14.4
	1th	30	3.2
Düzce-Bolu	3th	12	55.6
	2th	16	35.6
	1th	30	6.52
Kocaeli-Sakarya	3th	6	21.5
	2th	8	16.2
	1th	30	4.6

According to the simulations, the introduced variable orifice damping has a significant effect on the structural response. This effect, however, is of lower importance for damping coefficients larger than 5 N-s/mm. For higher values, the structural response is almost uneffected for all three earthqauke excitations. Table 3.1 and Table 3.2 prevent the minimum response values for the optimum damping coefficients. Although the response values of the three stories are not a minumum for different damping coefficients, the magnitude does not change significantly.

3.3. State Space Formulation of the Building

The equations of motion of the 3-story structure are given by Eq(1.1). The three-storey model structure with a variable damper is subjected to external excitation that enters the structure from the ground. The equation of motion can be written in the following state-space form :

$$\dot{x} = A\,x + B_1\,\ddot{u}_g + B_2\,f \tag{3.1}$$

$$z = C_1 x + D_{12} f \tag{3.2}$$

$$y_m = C_2 x + D_{21} \ddot{u}_g + D_{22} f \tag{3.3}$$

where x is the state vector and is defined as

$$x = \begin{bmatrix} x_d \\ \dot{x}_d \end{bmatrix} \tag{3.4}$$

$\ddot{u}_g$ is a one-dimensional ground acceleration, f is the control force, y_m is the vector of measured outputs and z is the regulated output vector.The state space matrices are defined as follows,

$$A = \begin{bmatrix} 0 & I \\ -M^{-1}K & -M^{-1}C \end{bmatrix} \quad , \quad B_1 = \begin{bmatrix} 0 \\ \Lambda \end{bmatrix} \quad , \quad B_2 = \begin{bmatrix} 0 \\ M^{-1}\Gamma \end{bmatrix} \tag{3.5}$$

$$C_1 = \begin{bmatrix} H_1 \\ H_2 \\ 0 \end{bmatrix} \quad , \quad D_{12} = \begin{bmatrix} E_1 \\ E_2 \\ R \end{bmatrix} \tag{3.6}$$

$$C_2 = \begin{bmatrix} I & 0 \\ 0 & I \\ -M^{-1}K & -M^{-1}C \end{bmatrix} \quad , \quad D_{21} = \begin{bmatrix} 0 \\ -\Lambda \end{bmatrix} \quad , \quad D_{22} = \begin{bmatrix} 0 \\ -M\Gamma \end{bmatrix} \tag{3.7}$$

where H_1 , H_2 and E_1 , E_2 are the fourth and sixth row of the state matrix A and B, respectively. The matrixes C_1 and D_{12} in the state vector z are adjusted to reduce the accceleration values of the first and third story. R is a positive coefficient reflecting the relative importance of the control force the acceleration values of the first and third story. The selection of the positive coefficient R according to the demand of the control system is explained in the following section.

3.4. Control Algorithm Development

The design of a linear quadratic regulator (LQR), a kalman filter estimator, and the closed feedback simulation of the three-storey model structure are the subjects of this section. The first step is to develop the design procedure for finding the LQR control method, the second step is to design the kalman filter estimator and the last is to apply the LQR based controller to the three-storey model structure.

The LQR method is used to obtain an optimum gain matrix K_{lqr} by minimizing a performance index J. In this study, the following performance index is used:

$$J = \int_{t=0}^{\infty} z^T * z \tag{3.8}$$

$$z = \begin{bmatrix} H_1 \\ H_2 \\ 0 \end{bmatrix} x + \begin{bmatrix} E_1 \\ E_2 \\ R \end{bmatrix} u \tag{3.9}$$

$$z^T z = \begin{cases} x^T [H_1{}^T H_2{}^T 0] \begin{bmatrix} H_1 \\ H_2 \\ 0 \end{bmatrix} x + x^T [H_1^T H_2^T O] \begin{bmatrix} E_1 \\ E_2 \\ R \end{bmatrix} u \\ + u^T [E_1{}^T E_2{}^T R^T] \begin{bmatrix} E_1 \\ E_2 \\ R \end{bmatrix} u + u^T [E_1{}^T E_2{}^T R^T] \begin{bmatrix} E_1 \\ E_2 \\ R \end{bmatrix} u \end{cases} \tag{3.10}$$

Control force is applied to first story. Thus,

$$E_1 = 10 \quad \text{, (first story)} \tag{3.11}$$

$$E_2 = 0 \quad \text{,(second story)} \tag{3.12}$$

If control force is applied to third story, we obtain,

$$Z=\begin{bmatrix} H_1 \\ 0 \end{bmatrix} x+\begin{bmatrix} 0 \\ R \end{bmatrix} u \tag{3.13}$$

$$z^T z=x^T \underbrace{H_2^T H_2}_{Q} x+u^T \underbrace{R^T R}_{\underline{R}} \tag{3.14}$$

As a result, K_{lqr} is the state feedback gain matrix that is given by

$$K_{lqr}=\underline{R^{-1}} B^T P \tag{3.15}$$

where P is a positive matrix called the Riccati matrix. It is obtained by solving the following Algebraic Riccati Equation (ARE):

$$Q+PA+A^T P-PBR^{-1} B^T P=0 \tag{3.16}$$

After minimizing the performance index factor J, the control force, f, is obtained as

$$f=K_{lqr} x_e \tag{3.17}$$

where x_e is the estimated state vector.

The design procedure for finding the LQR feedback K_{lqr} is:

- •Minimize the performance index factor J
- •By solving the algebraic Riccati equation for P
- •Find the state feedback gain matrix using $K_{lqr}=R^{-1} B^T P$

There are very good numerical procedures for solving the ARE. The SCILAB command that performs this is named lqr(P12).In the Scilab code,P12 represents the plant (continous time). (see Appendix A)

3.4.1. Choice of Positive Coefficient in Design of the LQR Control

The positive coefficient R is selected by the design engineer. Depending on how is design parameter is selected, the closed-loop system will give a different response. Hence our aim in this section is to develop efficient design parameter R to obtain the best reduction of the displacements, velocities and accelerations of the three-storey model structure.

In order to make a choice among various positive coefficient possibilities, several simulations are done. In these simulations, R is taken as different values changed from 0.1 to 10 logarithmically. Maximum first and third story displacement, acceleration values and maximum control force values for El Centro, Düzce-Bolu and Kocaeli-Sakarya earthquake records are calculated by the use of each R values. The maximum first and third story displacements, accelerations values and maximum control force values for each earthquake records for R ranging from 0.1 to 10 are plotted in Figure 3.7-Figure 3.11.

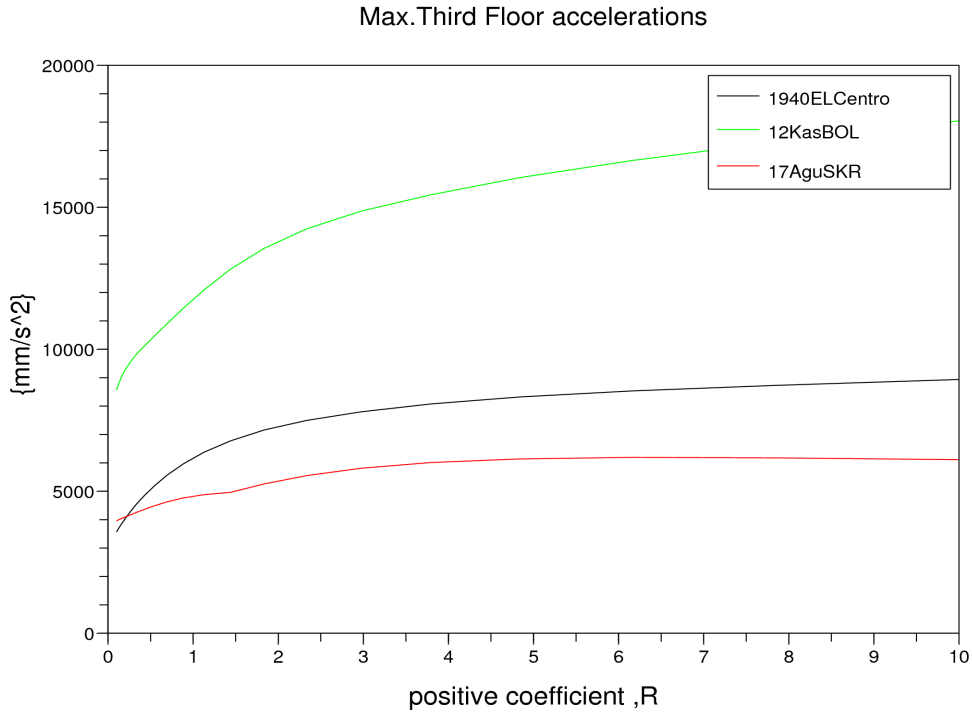

Figure 3.7. Maximum Third Floor Acceleration Values and R

Figure 3.7 indicates that maximum third floor acceleration values given earthquake records with the R ranging from 0.1 to 10, for R < 2 increasing R increases the maximum third story acceleration values while for R > 2 increasing the maximum third story acceleration values slightly.

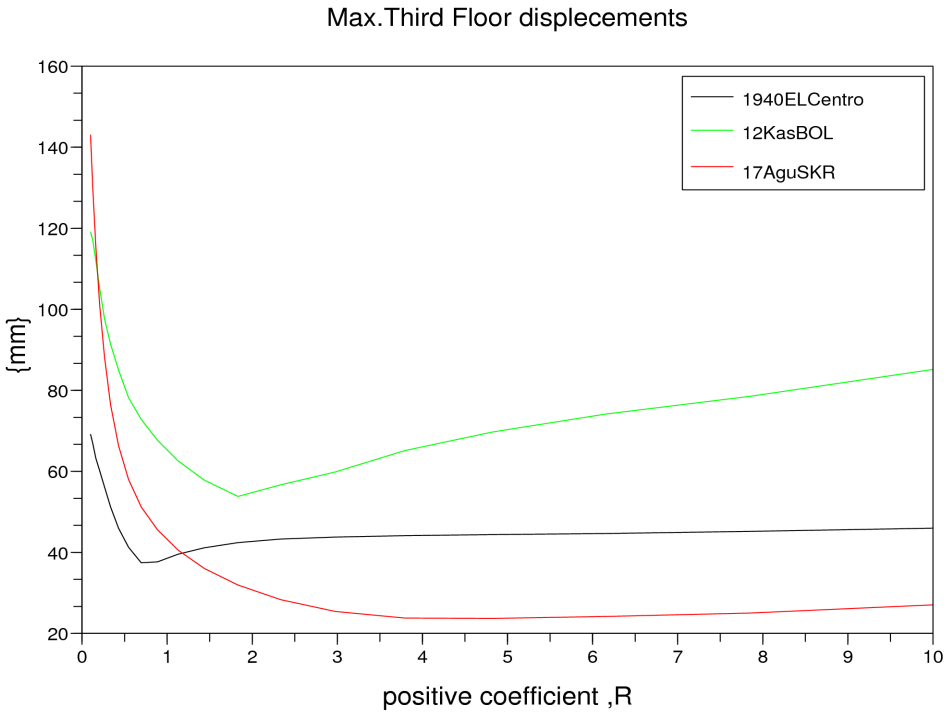

Figure 3.8. Maximum Third Floor Displacement Values and R

Figure 3.8 indicates that the maximum third story displacement values calculated using Kocaeli-Sakarya earthquake records with the R ranging from 0.1 to 10, increasing R decreases the maximum first story displacement values. Using the El Centro earthquake records, for R<0.7 increasing R decreases the maximum third story displacement values but R > 0.7 increasing R is not effective in reducing the maximum third story displacement values. In addittion, for the Düzce-Bolu earthquake records, for R < 1.8 increasing R decreases the maximum third story displacement values but for R > 1.8 increasing R increases the maximum third story displacement values.

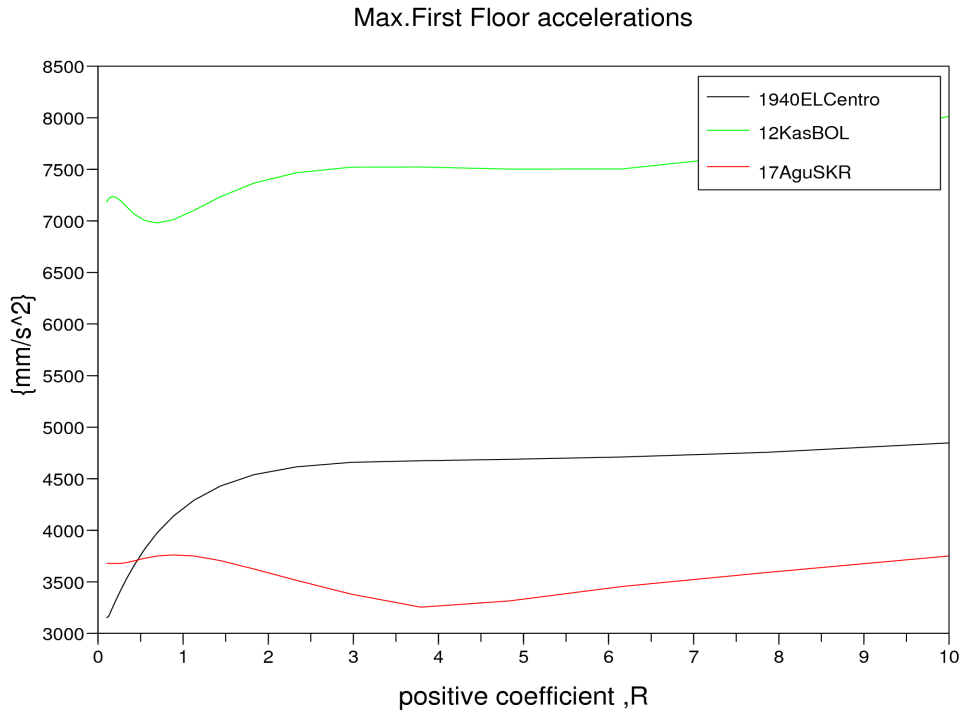

Figure 3.9. Maximum First Floor Acceleration Values and R

Figure 3.9 indicates that using the El Centro earthquake records with R < 1.5 and increasing R increases the maximum first story acceleration values, while for R > 1.5, the maximum first story acceleration values increase slightly. The maximum first floor displacement values calculated using the Düzce-Bolu earthquake records, for R <0 .8 increasing R decreases the maximum first story acceleration values but for 0.8 < R < 3.5 increasing R increases the maximum first story acceleration values, for R >3 .5 increasing R is not effective in reducing the maximum first story acceleration values.In addition this graph, the maximum first floor displacement values calculated using the Kocaeli-Sakarya earthquake records, for R <3.8 increasing R decreases the maximum first story acceleration values while for R >3.8 increasing R increases the maximum first story acceleration values.

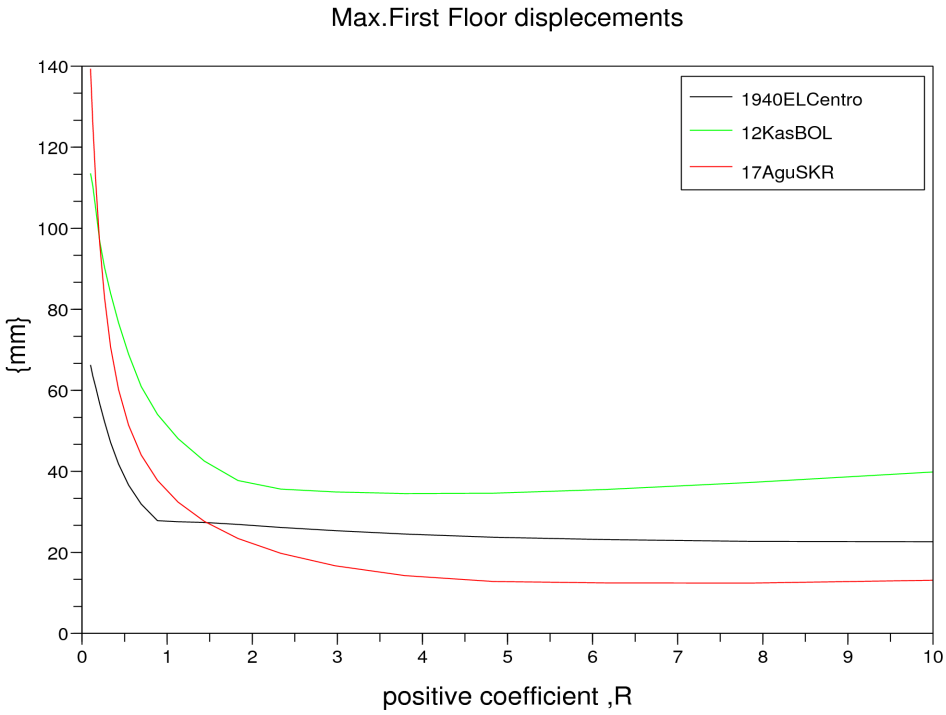

Figure 3.10. Maximum First Floor Displacement Values and R

Figure 3.10 indicates that the maximum first floor displacement values calculated using the El Centro earthquake records, for R < 0.9 increasing R decreases the maximum first story displacement values while for R > 0.9 decreasing the maximum first story displacement values sligthly. The maximum first floor displacement values calculated using Düzce-Bolu and Kocaeli-Sakarya earthquake records, for R<2 increasing R decreases the maximum first story displacement values but for R>2 increasing R is not effective in reducing the maximum first story displacement values.

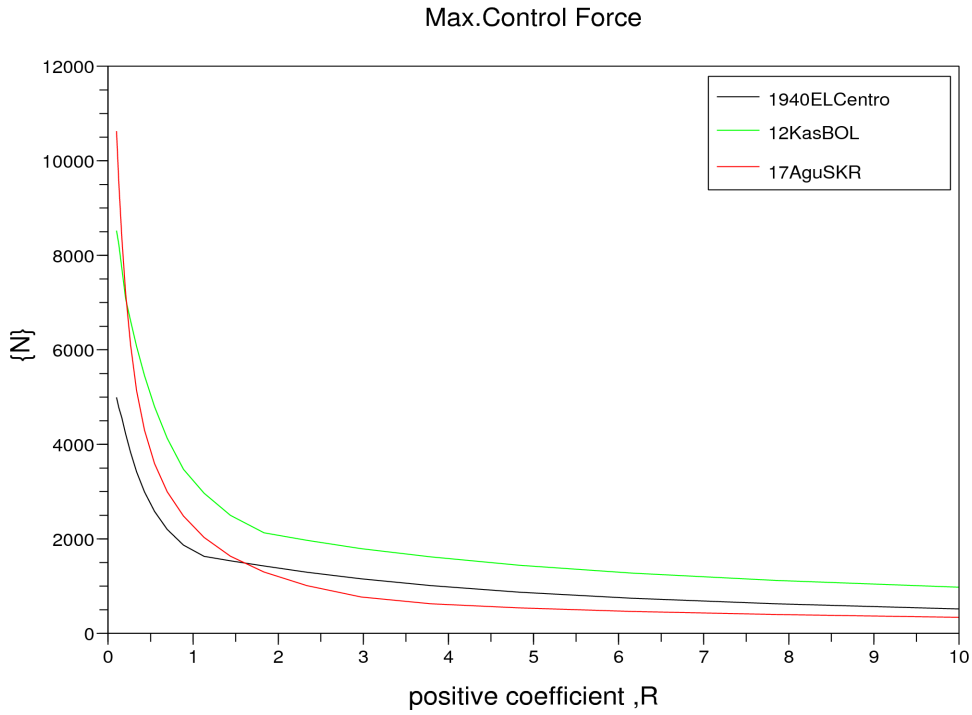

Figure 3.11. Maximum Control Force Values and R

Figure 3.11 shows the maximum control forces calculated using given earthquake records with R ranging from 0.1 to 10. For R<2 increasing R decreases the maximum control force values, while for R>2 increasing R decreases the maximum control force values slightly.

Finally, when these graphs are examined, it can be seen that R=2 is an optimum positive coefficient to reduce the response of the structure.

The corresponding feedback gain matrix is

$$K_{lqr} = [-\ 19.7242\ \ -5.99503\ \ 88.522\ \ 0.16541\ \ 1.16676\ \ -3.34623]$$

3.4.2. Kalman Filter Estimator Design

It is difficult to measure all the structural displacements and velocities directly in full scale model structures. In this case, we assume that only the displacements are being measured. In order to obtain the structural velocities, we need to use a special process, which is known as the kalman filter estimator. The design of the kalman filter estimator and using the resulting system to calculate structural velocities are the subjects of this section.

As seen in Sec.3.3, the state of a system is described by the set of first-order differential equations in the following form :

$$\dot{x} = A\,x + B_1\,\ddot{u}_g + B_2\,f \tag{3.1}$$

$$y_m = C_2\,x + D_{21}\,\ddot{u}_g + D_{22}\,f \tag{3.3}$$

Figure 3.12 shows the basic controller diagram.

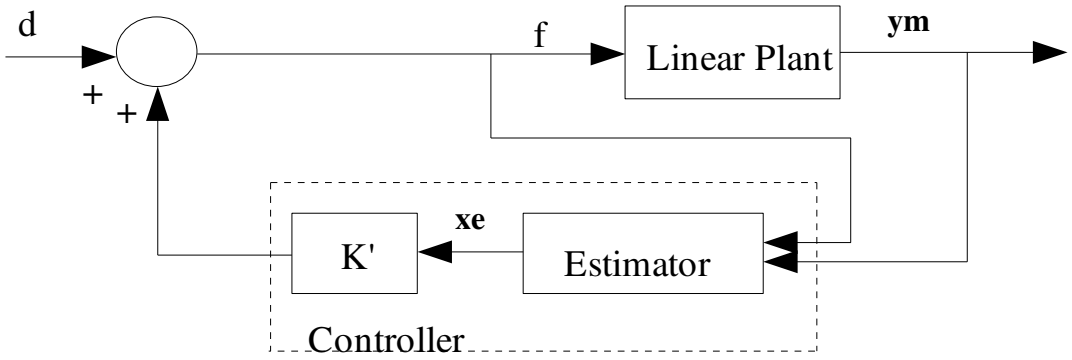

Figure. 3.12. The basic controller

The general concept of using the kalman filter estimator can be explained in the following way; the optimally estimated state vector of the system, x_e , can be obtained by using sensor measurements, y_m . For this study, structural velocities are defined as a optimum estimated state vector and sensor measurements are defined as structural displacements and structural accelerations (see Figure3.7).

The Kalman filter estimator is given by

$$\dot{x_e} = A x_e + B_1 d + B_2 f + K_e (y_e - y_m) \tag{3.18}$$

where K_e is the full measurement feedback gain matrix, and $y_e = C_2 x_e$ is the estimated output vector.

The control law is of the form

$$f = K_{lqr} x_e \tag{3.19}$$

Substituting Eq.3.19 into Eq.3.20 results in the following

$$\dot{x_e} = A x_e + B_1 d + B_2 (K_{lqr} x_e) + K_e (y_e - y_m) \tag{3.20}$$

Substituting $y_e = C_2 x_e$ into Eq.3.21 yields

After necessary manipulations, the kalman filter estimator is obtained in the following form:

$$\dot{x_e} = (A + B_2 K_{lqr} + K_e C_2) x_e + B_1 d - (K_e y_m) \tag{3.21}$$

As a result, structural velocities that can not be measured directly, can be calculated by using Eq.3.15. Figure 3.13, Figure 3.14 and Figure 3.15 show the estimated velocity response of the third, second and first floor of the three-story model structure, respectively.

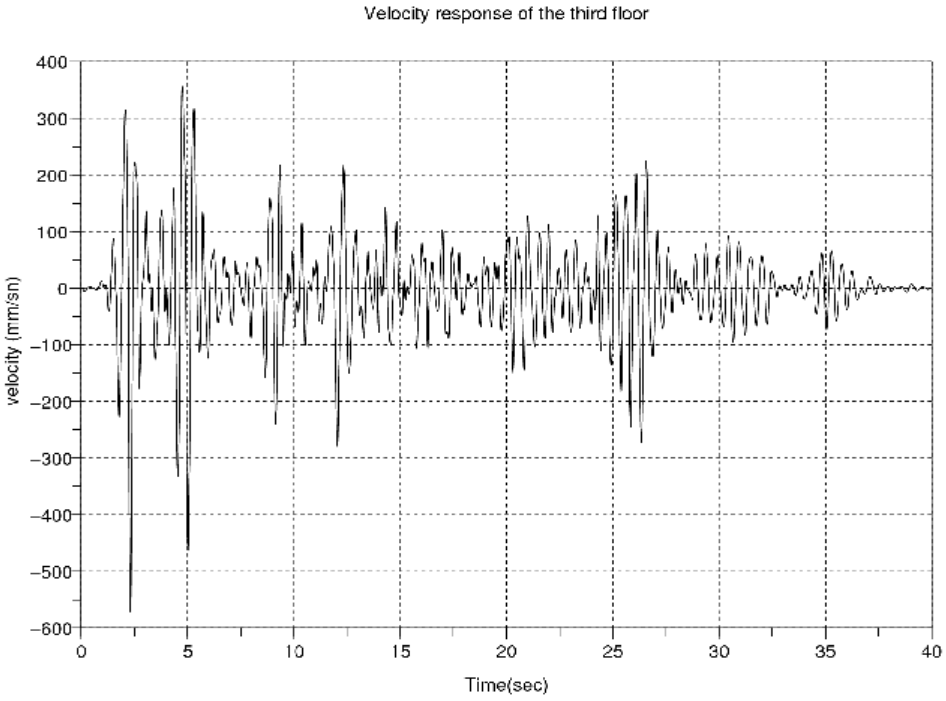

Figure 3.13. Velocity response of the third floor

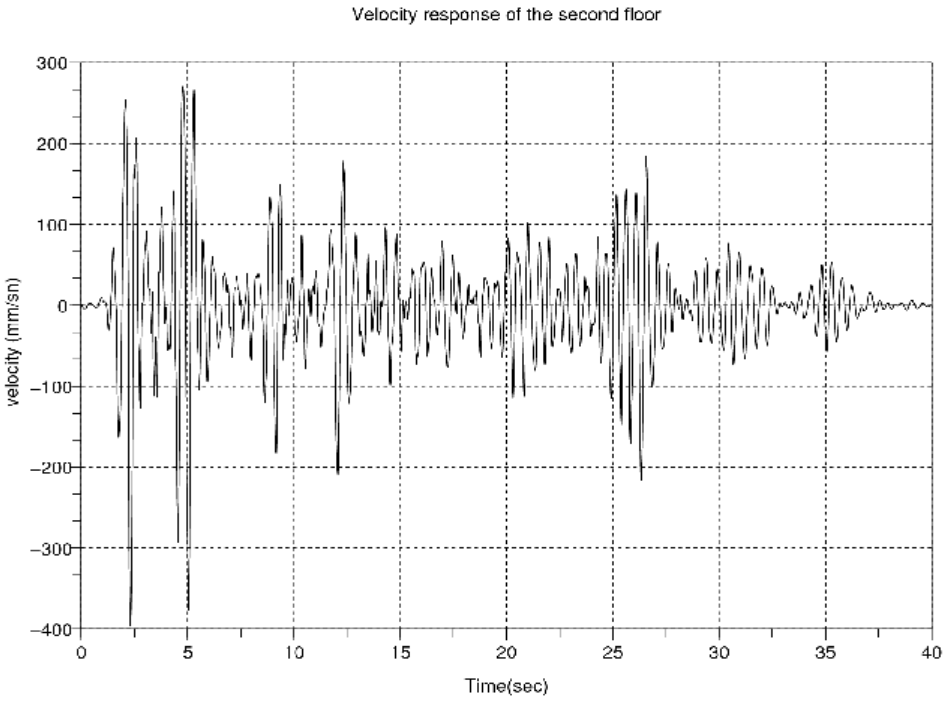

Figure 3.14. Velocity response of the second floor

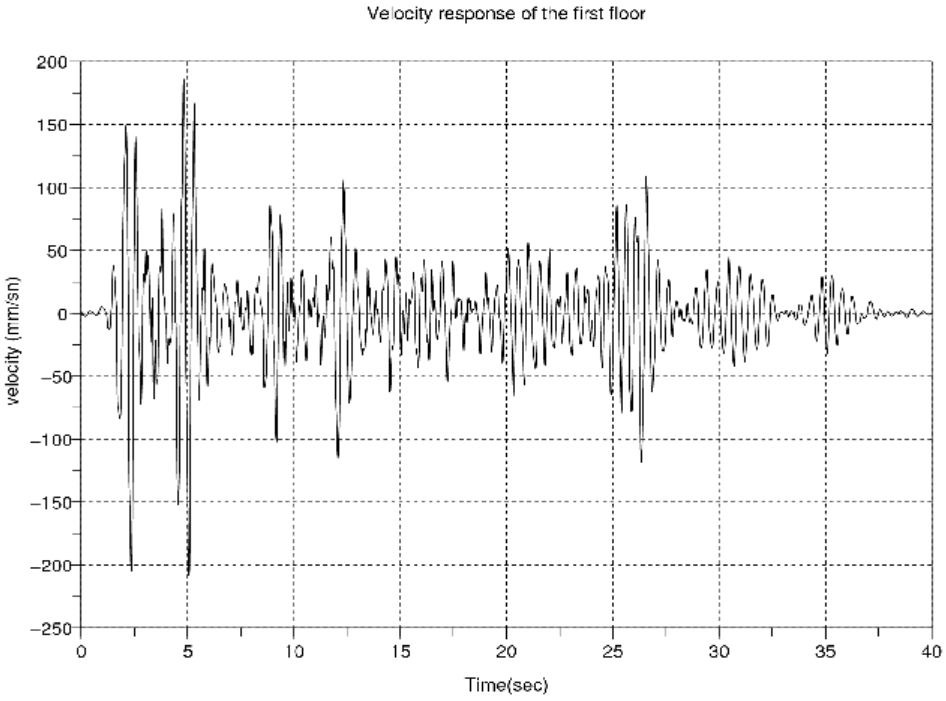

Figure 3.15.Velocity response of the first floor

3.5. Block Diagram of the Semi-Active Control System

A block diagram of the semi-active control system is shown in Figure 3.16. In the diagram, f is the force produced by the damper, $\dot{x}_{e1}$ is the estimated velocity response of the first floor, x_{m1} is the real velocity of the first floor. In the block diagram, the dependence of the semi-active damper on the structural response is determined by the velocity response of the first floor.

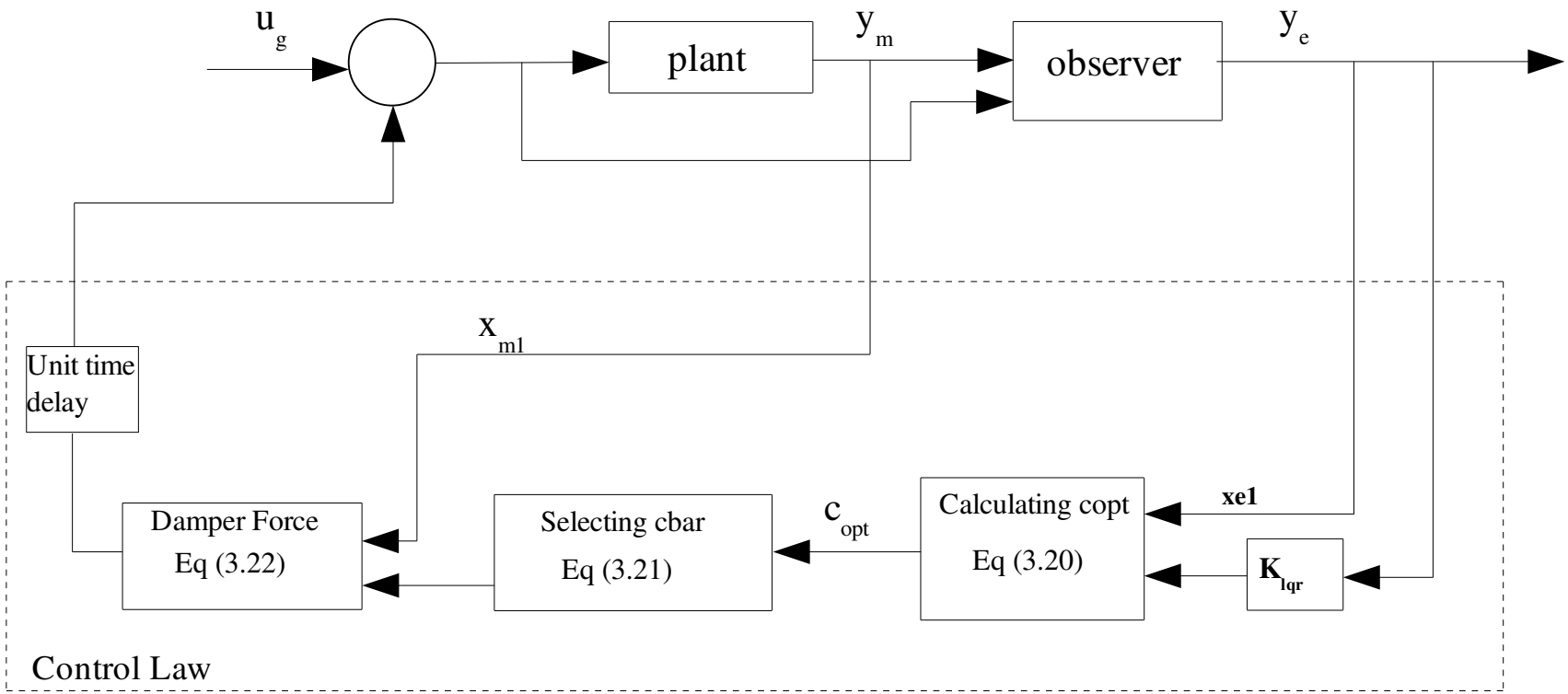

Figure 3.16. Block Diagram of the Semi-Active Control System.

3.6. Scicos Model of the Semi-Active Control System

SCICOS, a visual block simulation software that is based on Scilab is used to simulate features and limitations of the semi-active control algorithm. The three-storey model structure connected to sensors, control devices, A\D converter, D\A converter and semi-active control algorithm are modeled and interconnected in the block diagram shown in Figure 3.14. A time delay of 0.01 seconds is added to the application of the control force. This will account for the delay caused by the measurement, conversion of data, computations, and finally activation of the damper force. The scicos model of the semi-active control system is illustrated in Figure 3.21.

3.6.1. Sensors

A full state feedback control system requires the values of the states at each time step. The states, which are simply the structural displacements and velocities of the 3 story structure are not accessible directly. While displacements can be obtained easily by using potentiometers, velocities, on the other hand, are not obtainable directly. In this study, they are calculated by an observer by using feedback from the structural displacements.For this purpose, the relative displacements with respect to the shaking table are measured. (see Figure 3.17).

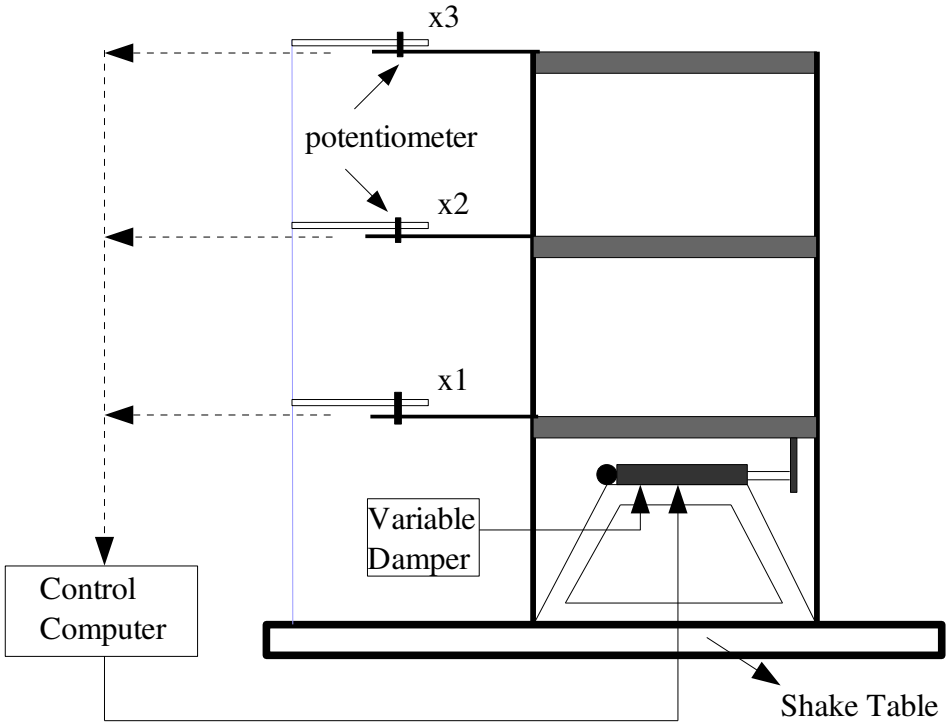

Figure 3.17. The position of potentiometers

The potentiometers were determined to have a sensitivity of 10 volts/55.10 mm.The value of the 55.1 mm is the maximum value of the third strory displacement.

The sensor output is described as

$$ys = D_s y_m + v \tag{3.22}$$

where y_m is the vector of measurement responses in Volts, $D_s = \frac{10}{55.10}\frac{volts}{mm}$, y_s is the vector of measurement displacements of each floor which is dependent on the selected measurement devices. D_s was selected to the absolute maximum and minumum value of the y_s would not exceed 10 Volts.

3.6.2. A/D Converter and D/A Converter

An analog to digital converter (A/D) is a device that converts an analog input voltage to a digital number. The digital to analog (D/A) converter simply does the opposite of an A/D. In this study, the A/D and D/A converters have 12-bit precision and a span of ± 10 V. These converters are modeled by a quantization and a saturation block (see Figure 3.19 and 3.20). In the A/D converter, the measured signal is digitized with respect to 12 bit precision. The second and final step is the saturation of the signal in the -10 and +10 interval as shown in Figure 3.10. Firstly, the digital signal received from the control computer is saturated in the same range as the D/A converter. Then it is digitized, again by an accuracy of 12 bits.

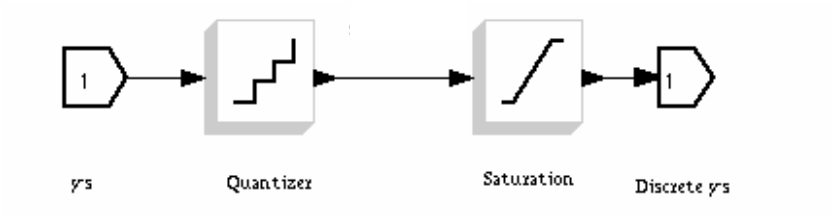

Figure 3.18. A/D Converter

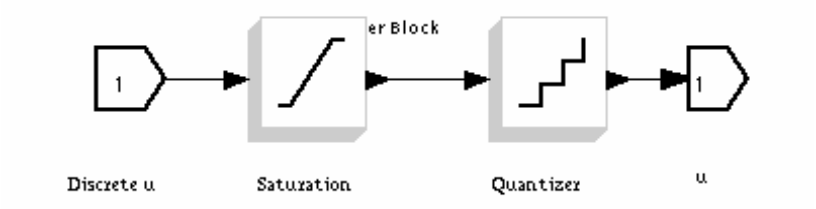

Figure 3.19. D/A Converter

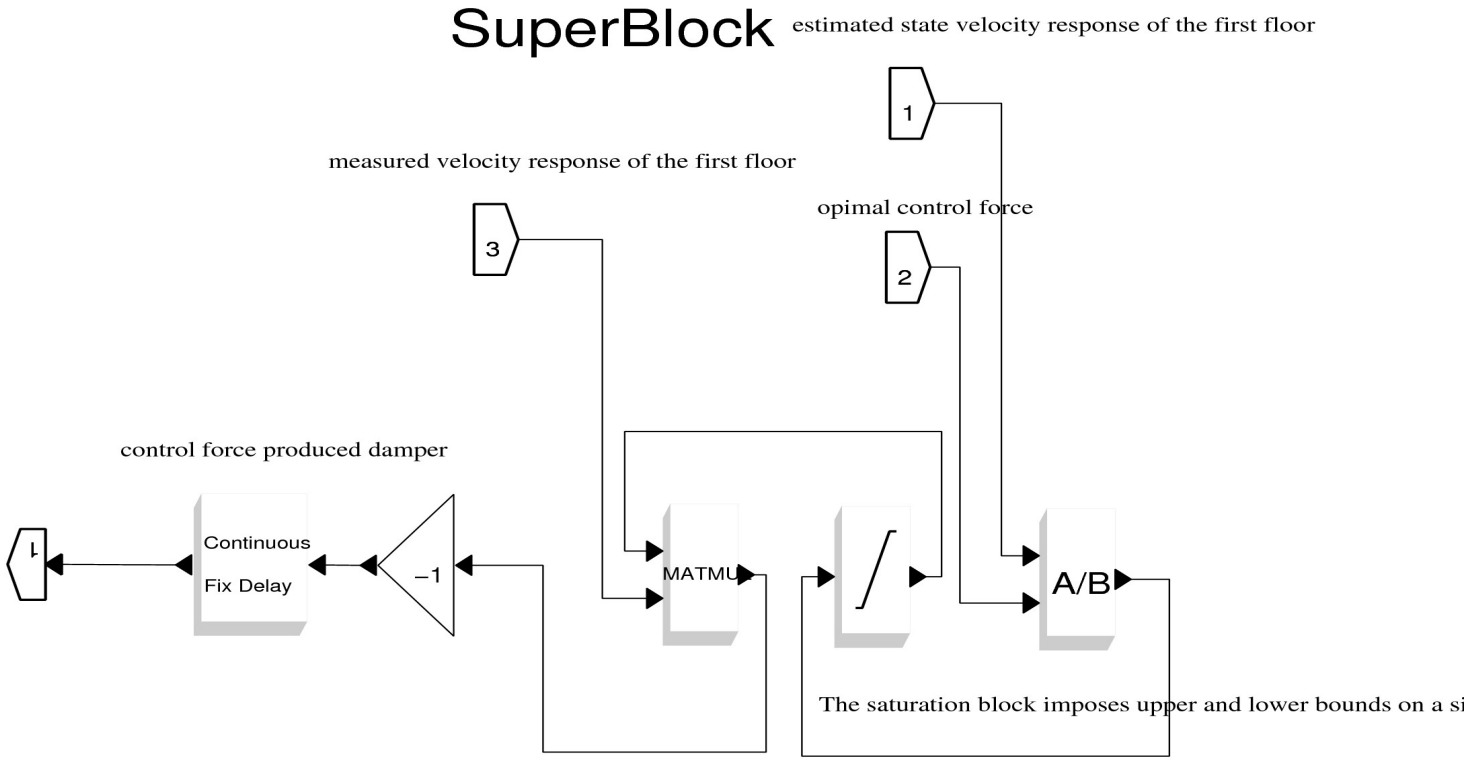

Figure 3.20. Scicos Model of the Damper Model

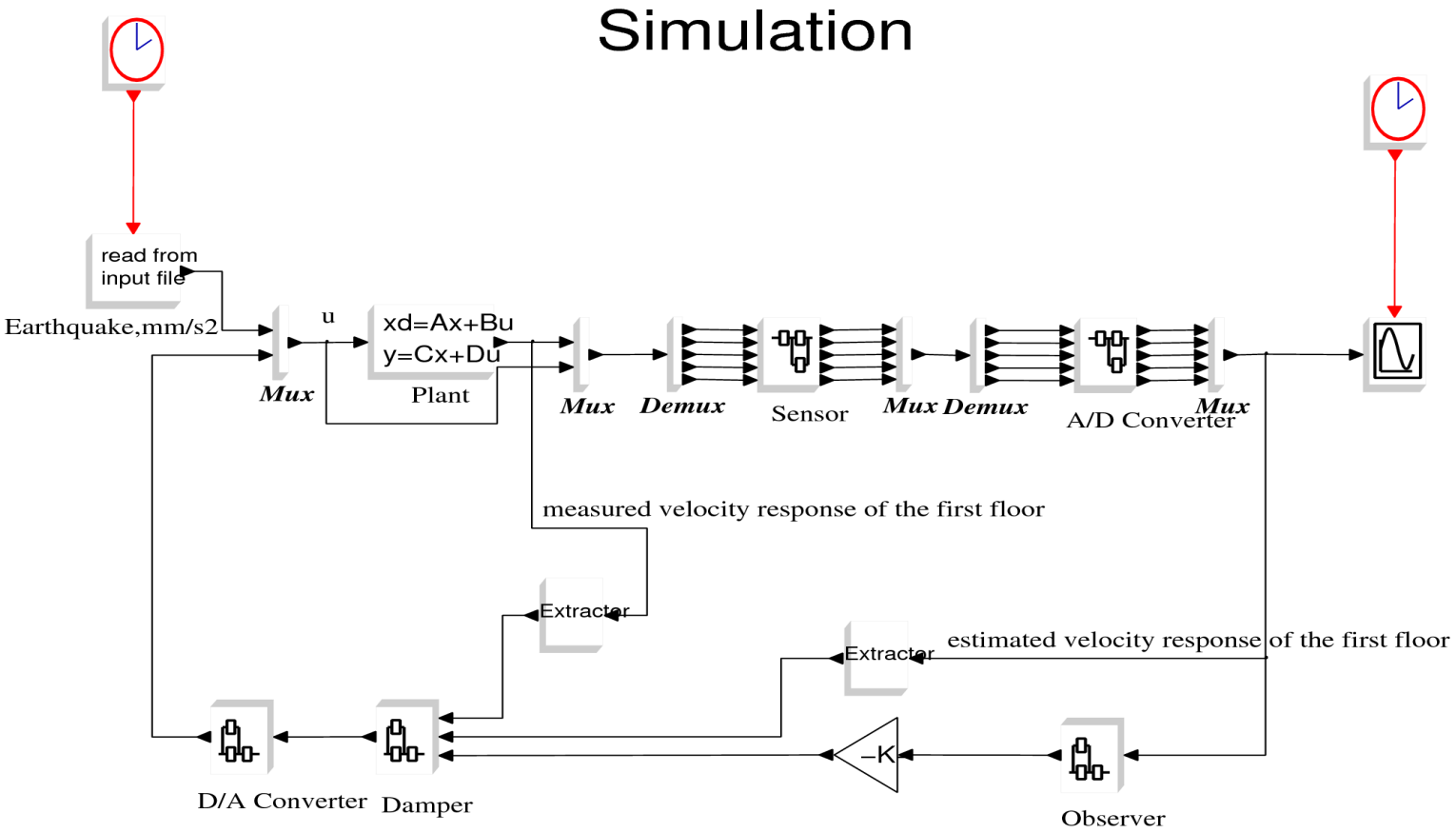

Figure 3.21. Scicos Model of the Semi-Active Control System

3.7. Control Devices

A variable orifice damper is utilized in this study to reduce the response of the three-storey model structure against earthquake loading. A number of researches including, a clipped optimal control algorithm (Sack 1994), a Linear Quadratic Regulator (LQR) algorithm (Symans and Constantinou 1995), a generalized LQR algorithm with a penalty on the acceleration response (Sadek and Mohraz 1998), have reveal that using variable dampers are effective in reducing the response of structures. In addition to this, these devices do not require large power source.

The damping coefficient, c(t), of the variable orifice damper, is selected between upper and lower limits, c_{max} and c_{min} ;

$$c_{min} \leq c(t) \leq c_{max} \tag{3.23}$$

In this study, minimum and maximum damping coefficients of the damper are selected as $c_{min} = 6.5\, N-sec/mm$ and $c_{max} = 30\, N-sec/mm$, respectively. The optimal damping coefficient of damper, $c_{opt}(t)$, at time t can be calculated from Equation (3.17) as

$$c_{opt}(t) = \frac{f(t)}{\dot{x}_{e1}} = \frac{K_{lqr} \times x_e}{\dot{x}_{e1}} \tag{3.24}$$

where $\dot{x}_{e1}$ is the relative velocity of the first floor. Using the constraints in Eq.(3.23), the damping coefficient to be assigned to the damper, $\bar{c}(t)$, is selected as

$$\bar{c}(t) = \begin{pmatrix} c_{min}, c_{opt}(t) < c_{min} \\ c_{opt}(t), c_{min} < c_{opt}(t) < c_{max} \\ c_{max}, c_{opt}(t) > c_{max} \end{pmatrix} \tag{3.24}$$

Finally,the control force can be calculated in the following way

$$f = \bar{c} \times \dot{x}_{m1} \tag{3.25}$$

3.8. The Results

In simulations,the three-story model structure is subjected to the NS component of the 1940 Imperial Valley, Kocaeli-Sakarya and Düzce-Bolu earthquake records obtained from the El Centro, Düzce, and Bolu stations, respecitvely (Fig 3.22-Fig 3.24). The relative displacements, relative velocities, and absolute acceleration time responses of the buildings third, second, and first floor are selected to compare controlled and uncontrolled responses of the structure. Table 3.3-Table 3.5 summarize the results of the maximum values of the controlled and uncontrolled responses of the structure. The relative displacements, relative velocities, and absolute acceleration time responses of the buildings third, second, and first floor are shown in Figure 3.25 - Figure 3.36.

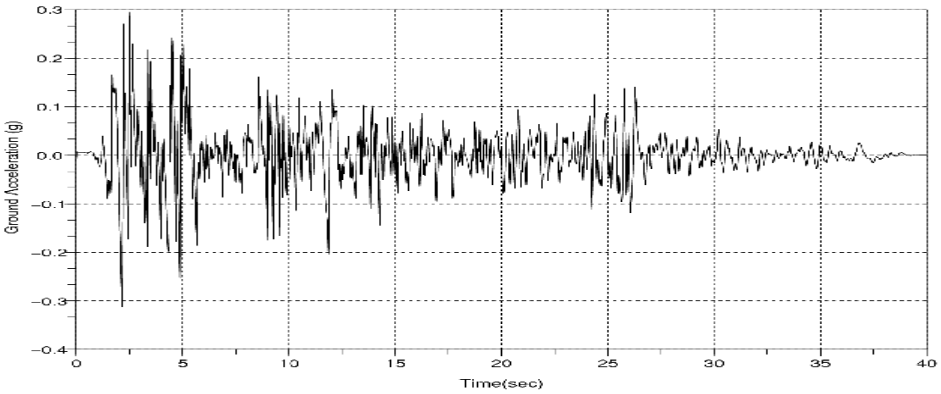

Figure 3.22. NS Component of the Ground Acceleration for the 1940 El Centro

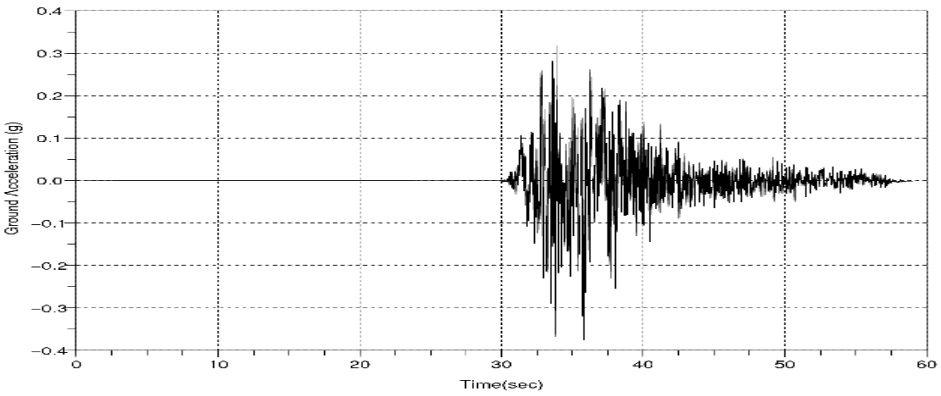

Figure 3.23. Ground Acceleration for the Sakarya

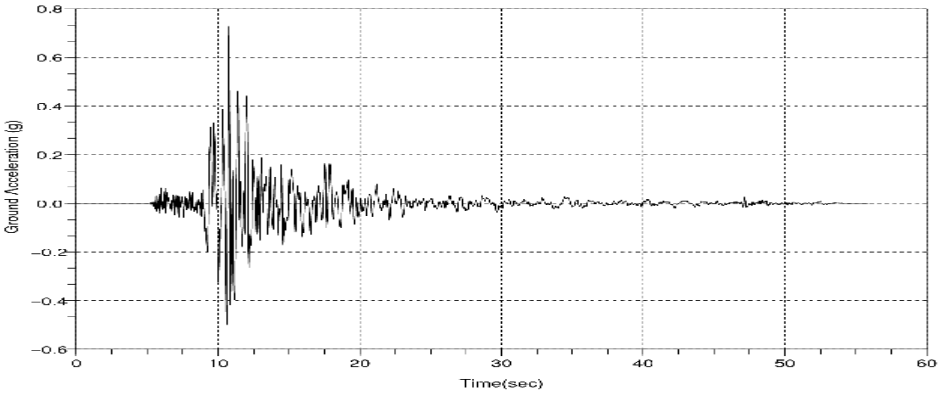

Figure 3.24. Ground Acceleration for the Düzce

Table 3.3. Maximum values of the controlled and uncontrolled responses of the structure for El Centro Earthquake

	Excitation	Story Number	Uncontrolled	Controlled	**%Reduction**
Displacements (mm)	El Centro	3 2 1	60.68 48.68 27.04	28.44 22.54 11.32	**%53.13** **%53.69** **%58.13**
Velocities (mm/s)		3 2 1	849.4 626.7 325.0	444.5 282.9 115.9	**%47.67** **%54.86** **%64.34**
Acceleration (mm/s2)		3 2 1	11490 9968 6097	6910 6289 3612	**%39.86** **%36.91** **%40.76**

Table 3.4. Maximum values of the controlled and uncontrolled responses of the structure for Düzce-Bolu Earthquake

	Excitation	Story Number	Uncontrolled	Controlled	**%Reduction**
Displacements (mm)	Düzce-Bolu	3 2 1	160 129 72.6	63.2 43.9 17.8	**%60.5** **%65.9** **%75.5**
Velocities (mm/s)		3 2 1	1970 1510 835	1050 729 259	**%46.7** **%51.7** **%68.9**
Acceleration (mm/s2)		3 2 1	24440 20200 12300	19600 13000 5320	**%19.8** **%35.7** **%56.7**

Table 3.5. Maximum values of the controlled and uncontrolled responses of the structure for Kocaeli-Sakarya Earthquake

	Excitation	Story Number	Uncontrolled	Controlled	**%Reduction**
Displacements (mm)	Kocaeli-Sakarya	3 2 1	39.4 30.7 17.2	21.3 14.4 7.14	**%45.9** **%53.1** **%58.4**
Velocities (mm/s)		3 2 1	425 448 290	294 212 93.4	**%30.8** **%52.7** **%62.8**
Acceleration (mm/s2)		3 2 1	9740 5870 6470	7320 4820 3380	**%24.8** **%17.9** **%47.8**

3.9. Conclusion

Semi-active control of a variable orifice damper has been successfully implemented in a three story model structure. Using the LQR control method, a stabilizing controller is found for the structure and the closed loop semi-active system is simulated by using three different earthquake records. It is illustrated by numerical simulations that semi-active control of a variable orifice damper is an effective methot to reduce the response of the structure.Reductions in the relative displacements, relative velocities, and absolute acceleration time responses of the buildings third, second, and first floor for the three earthquake records were observed with the semi-actively controlled systems. Reductions in the maximum acceleration values of the third floor for El Cenro, Düzce-Bolu and Kocaeli-Sakarya earthquake records are %40.76, %56.7, %47.8 respectively. To obtain the best performance from the semi-active control algorithm the positive coefficients, R, was selected carefully and the regulated output vector was determined according to the structural behaviour.

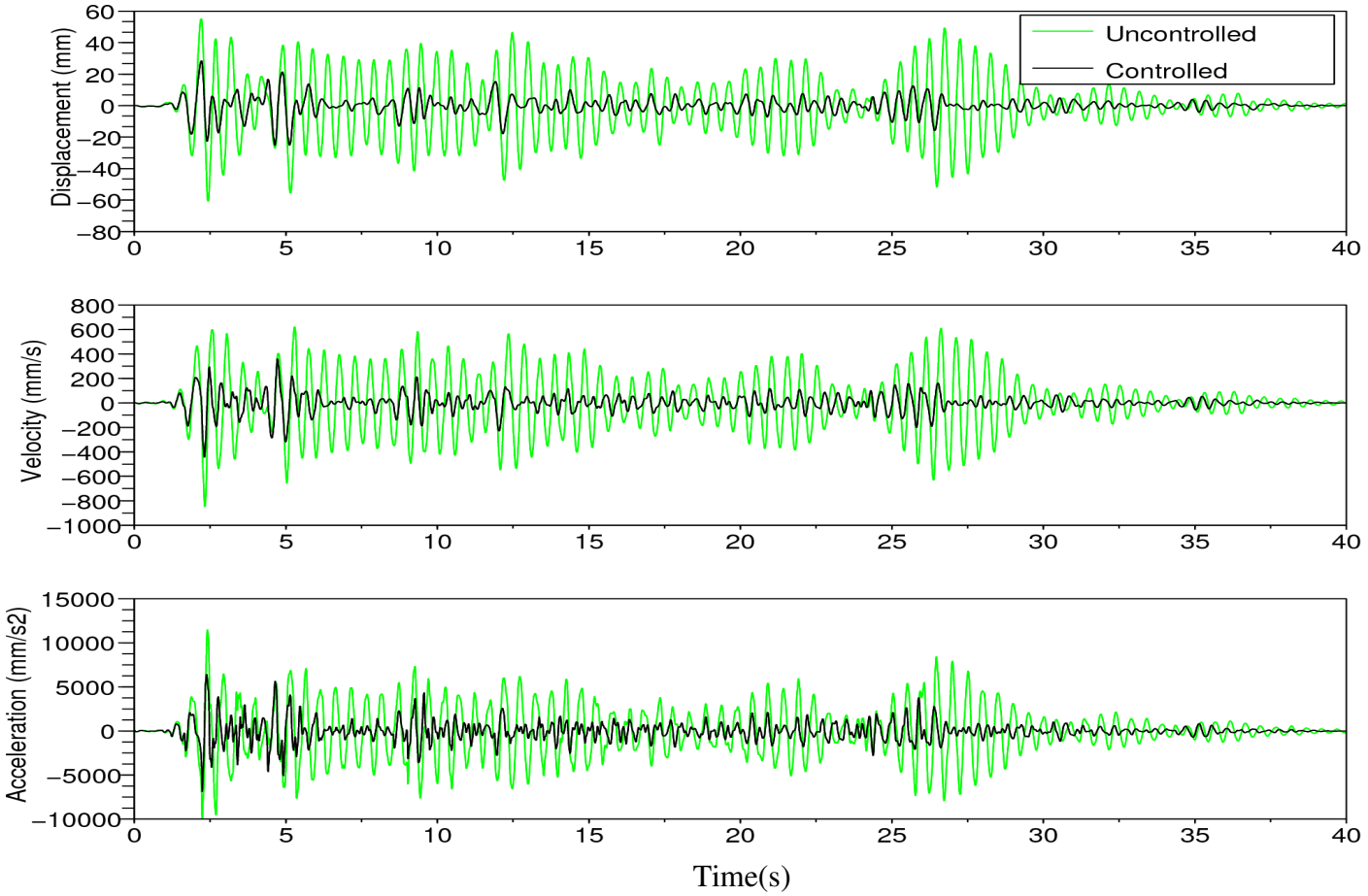

Figure 3.25. Time history of the third story of the model structure for El Centro Earthquake

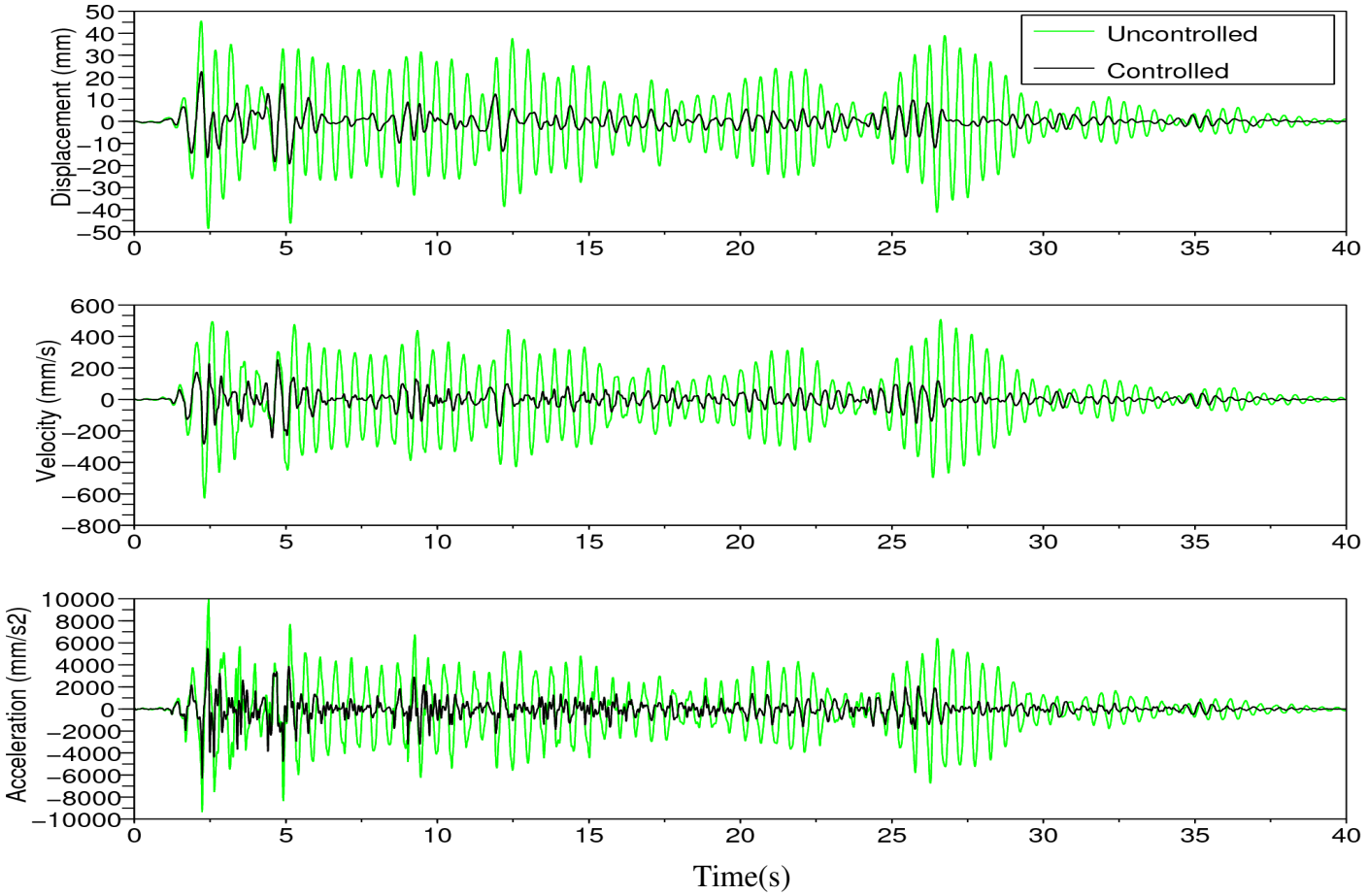

Figure 3.26. Time history of the second story of the model structure for El Centro Earthquake

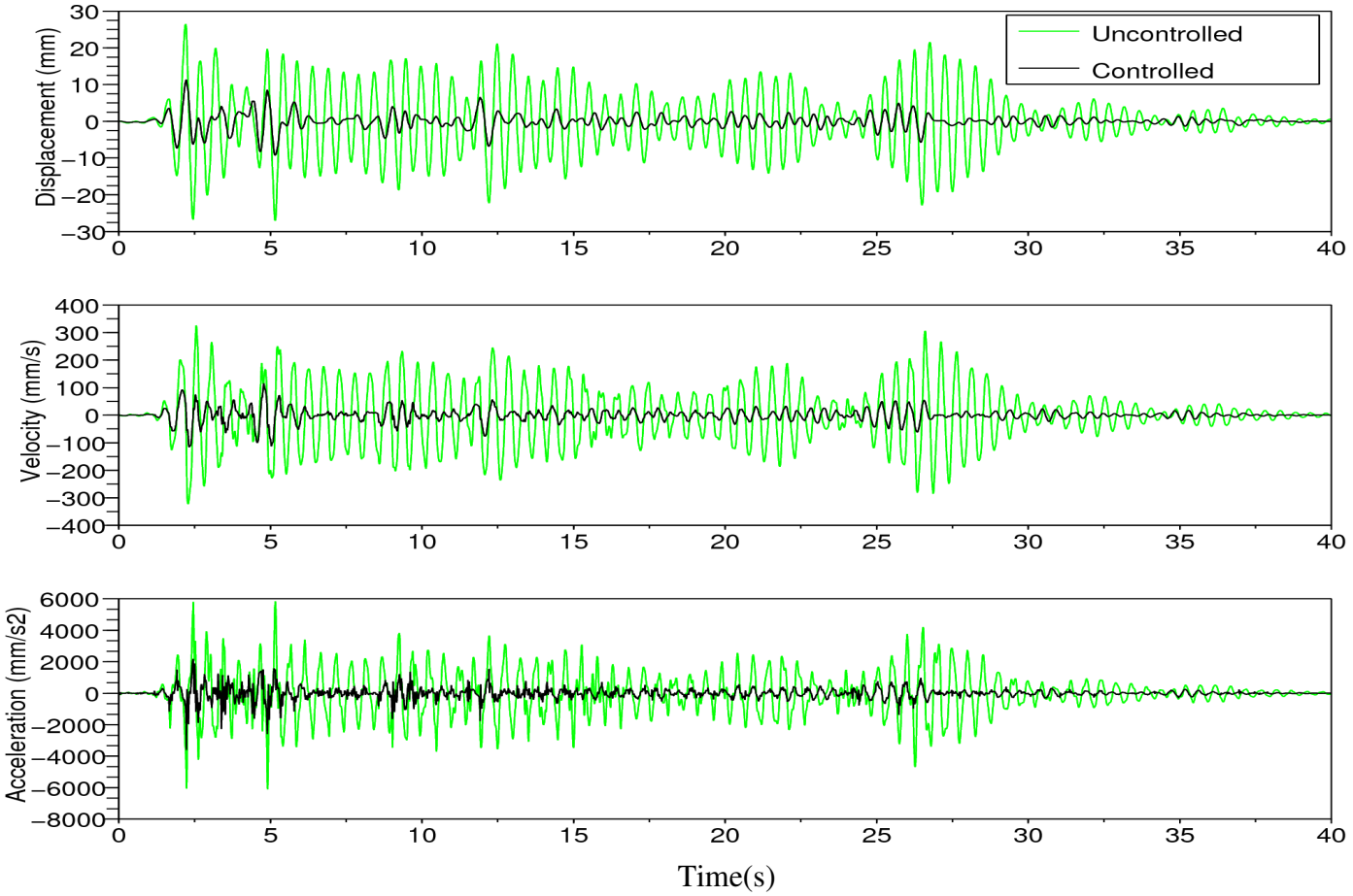

Figure 3.27. Time history of the first story of the model structure for El Centro Earthquake

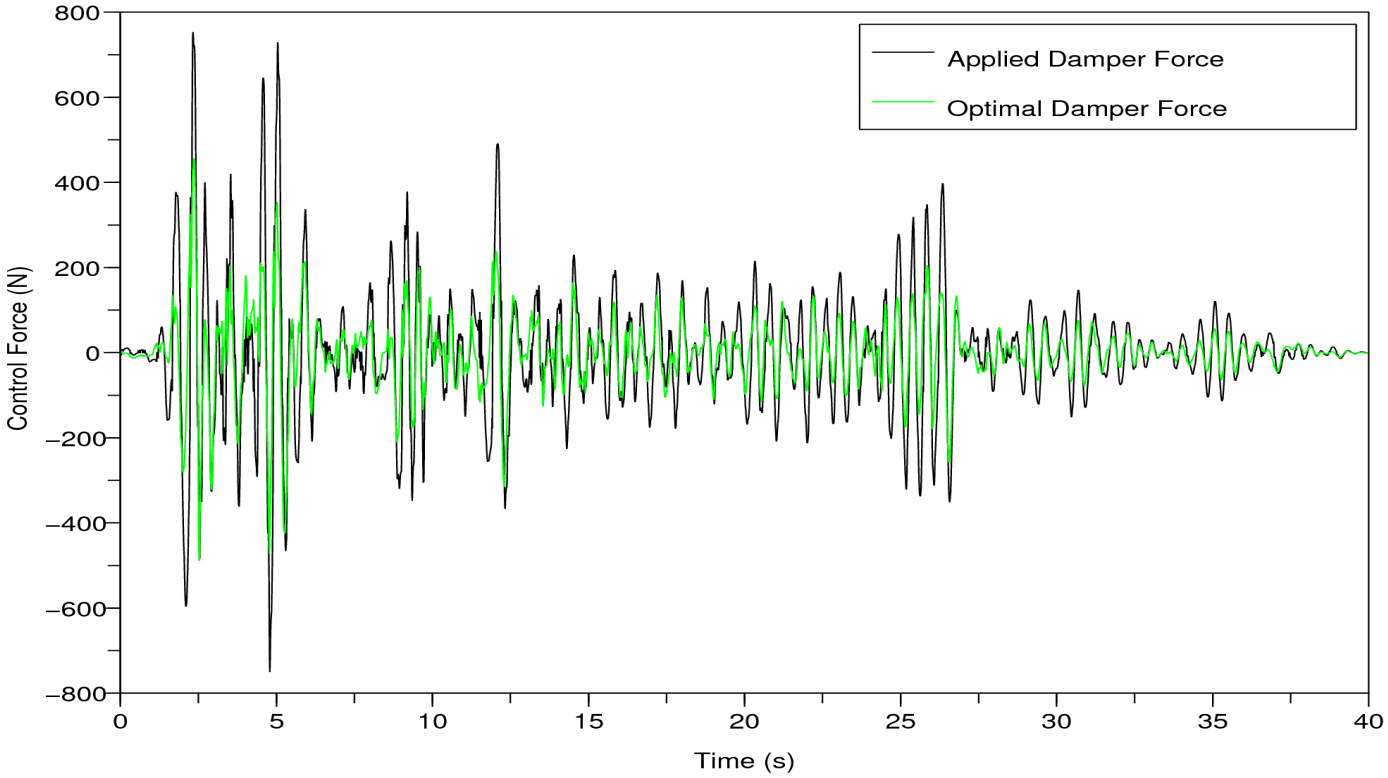

Figure 3.28. Control Force evaluated three story model structure for El Centro Earthquake

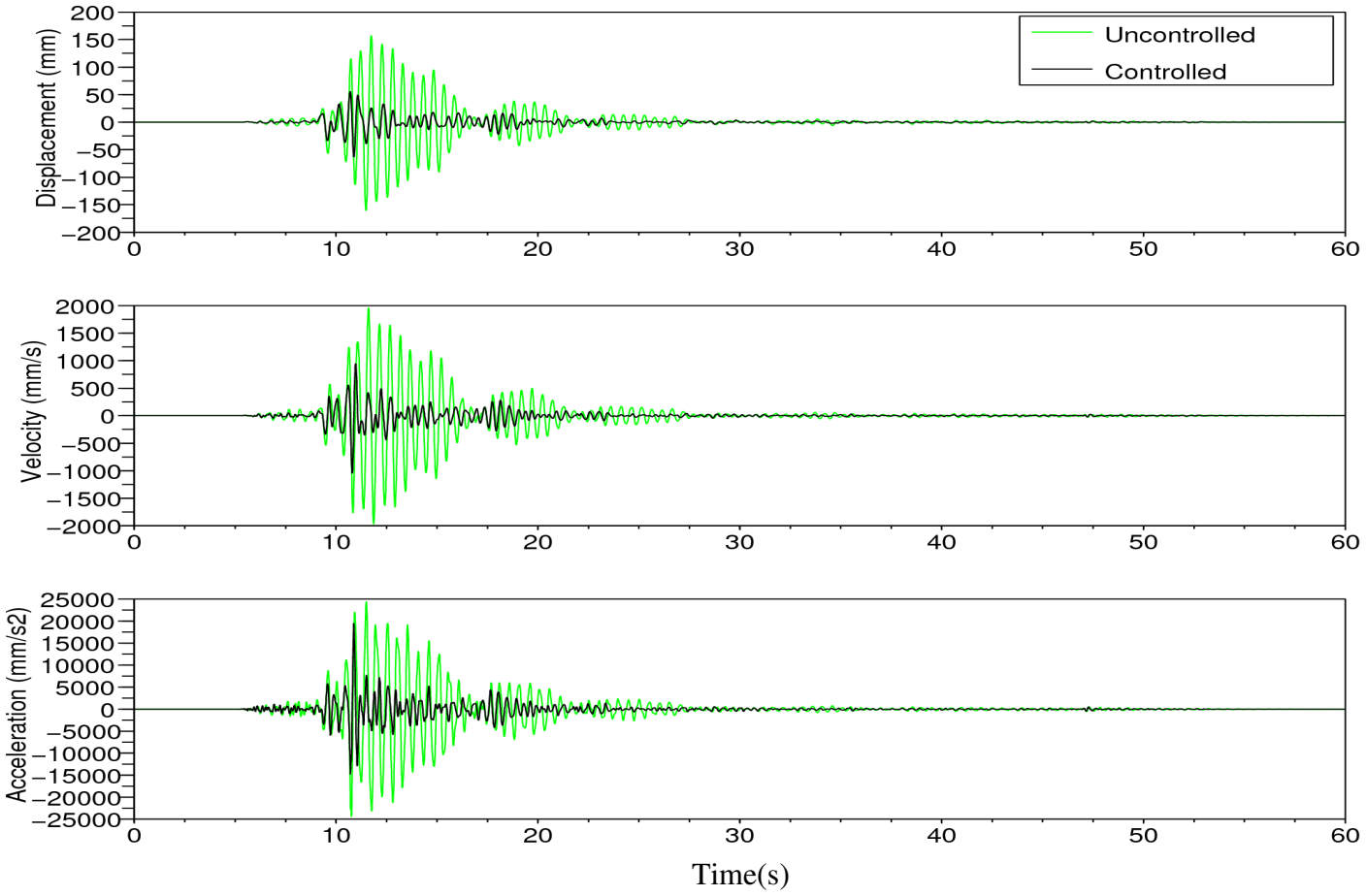

Figure 3.29. Time history of the third floor of the three story structure for Düzce-Bolu earthquake

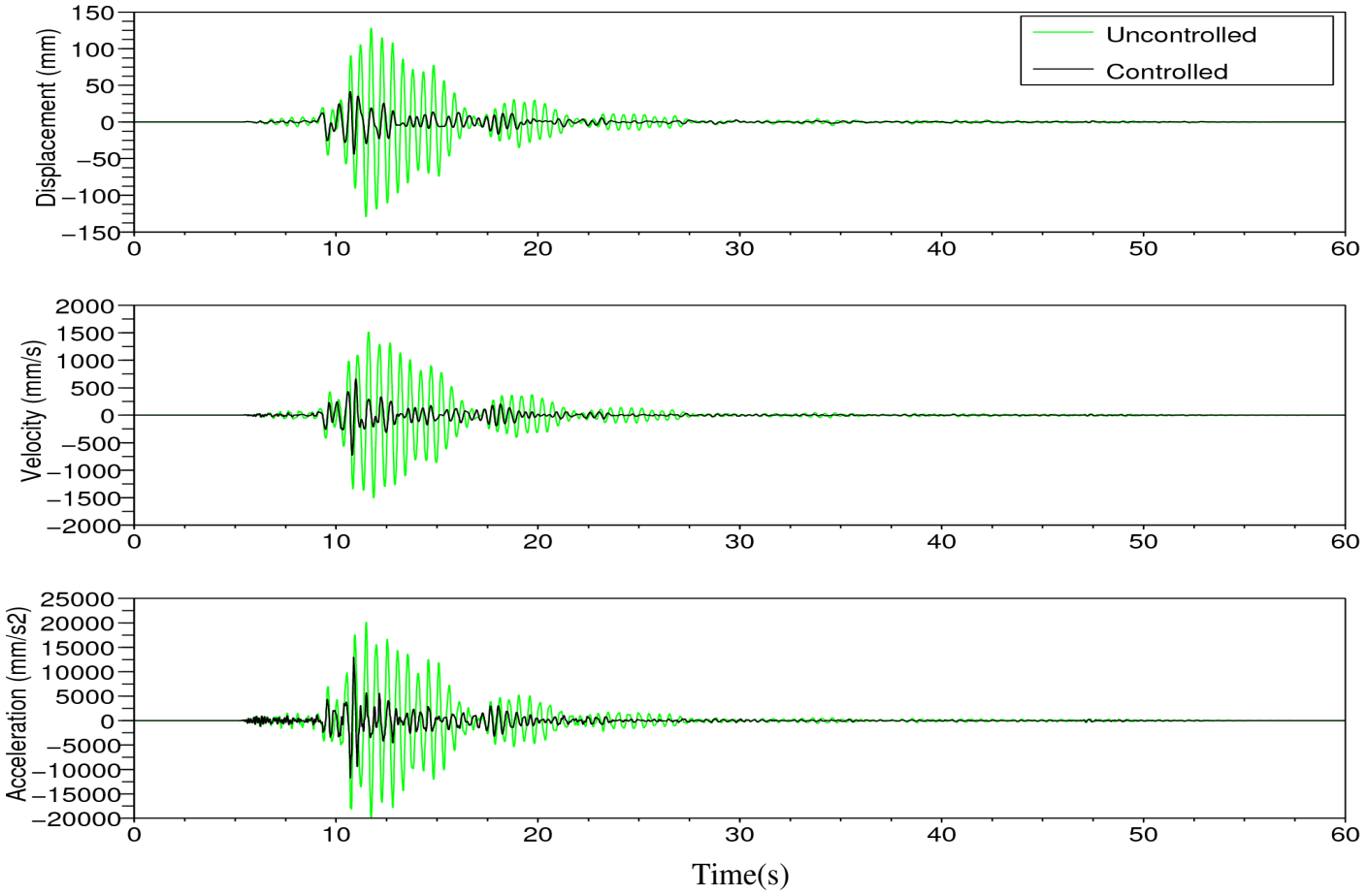

Figure 3.30. Time history of the third floor of the second story structure for Düzce-Bolu earthquake

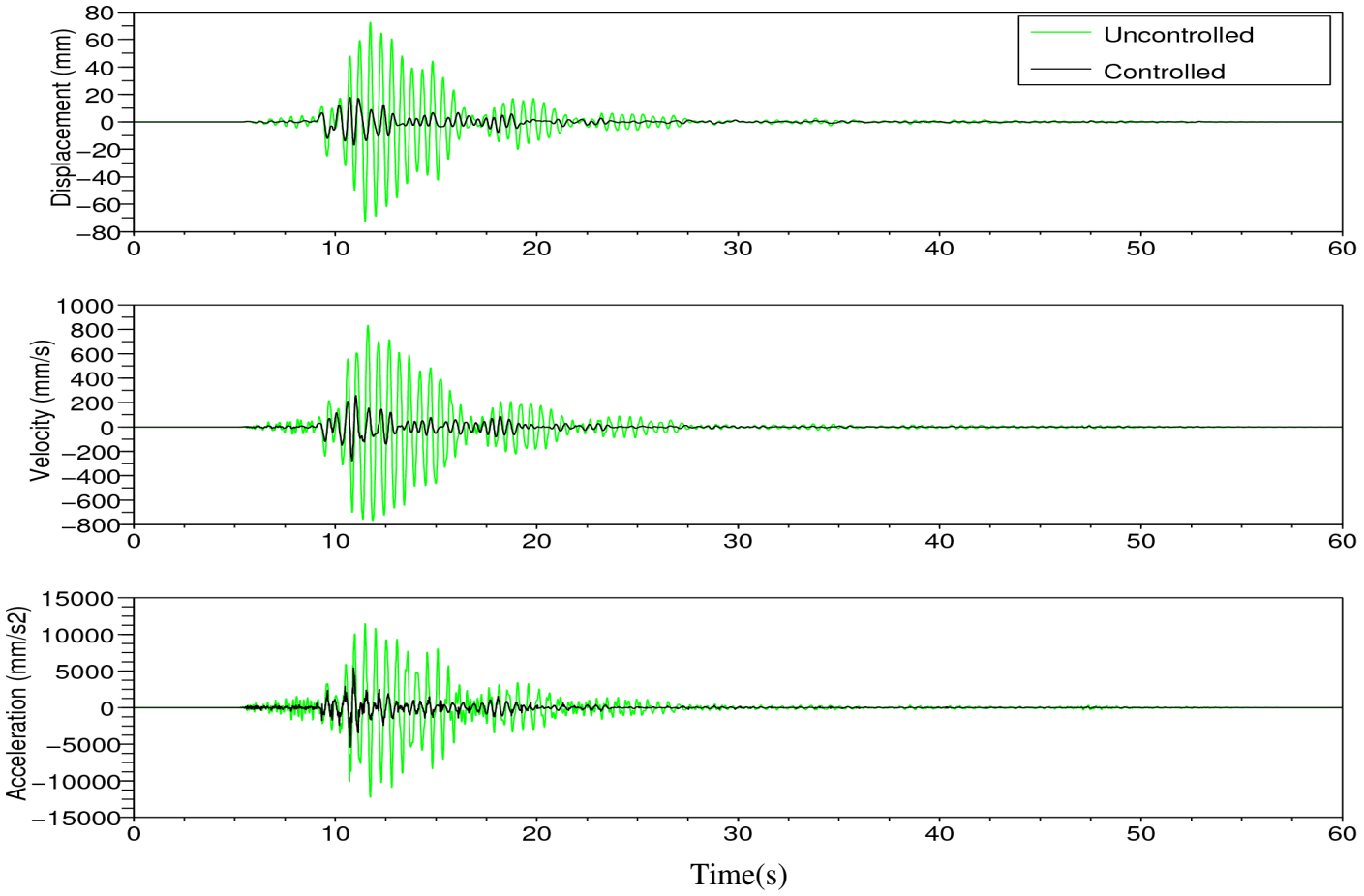

Figure 3.31. Time history of the first floor of the second story structure for Düzce-Bolu earthquake

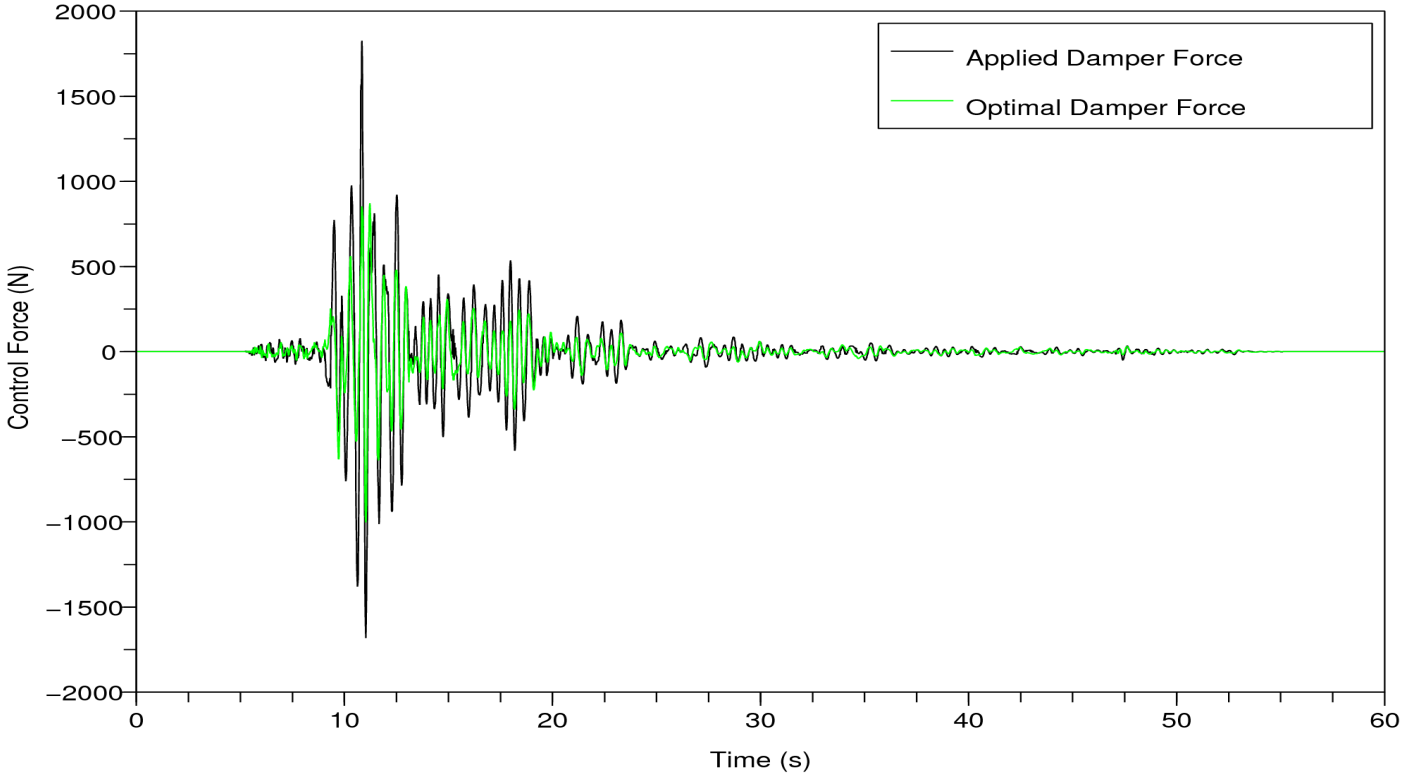

Figure 3.32. Control force evaluated three story structure for Düzce-Bolu earthquake

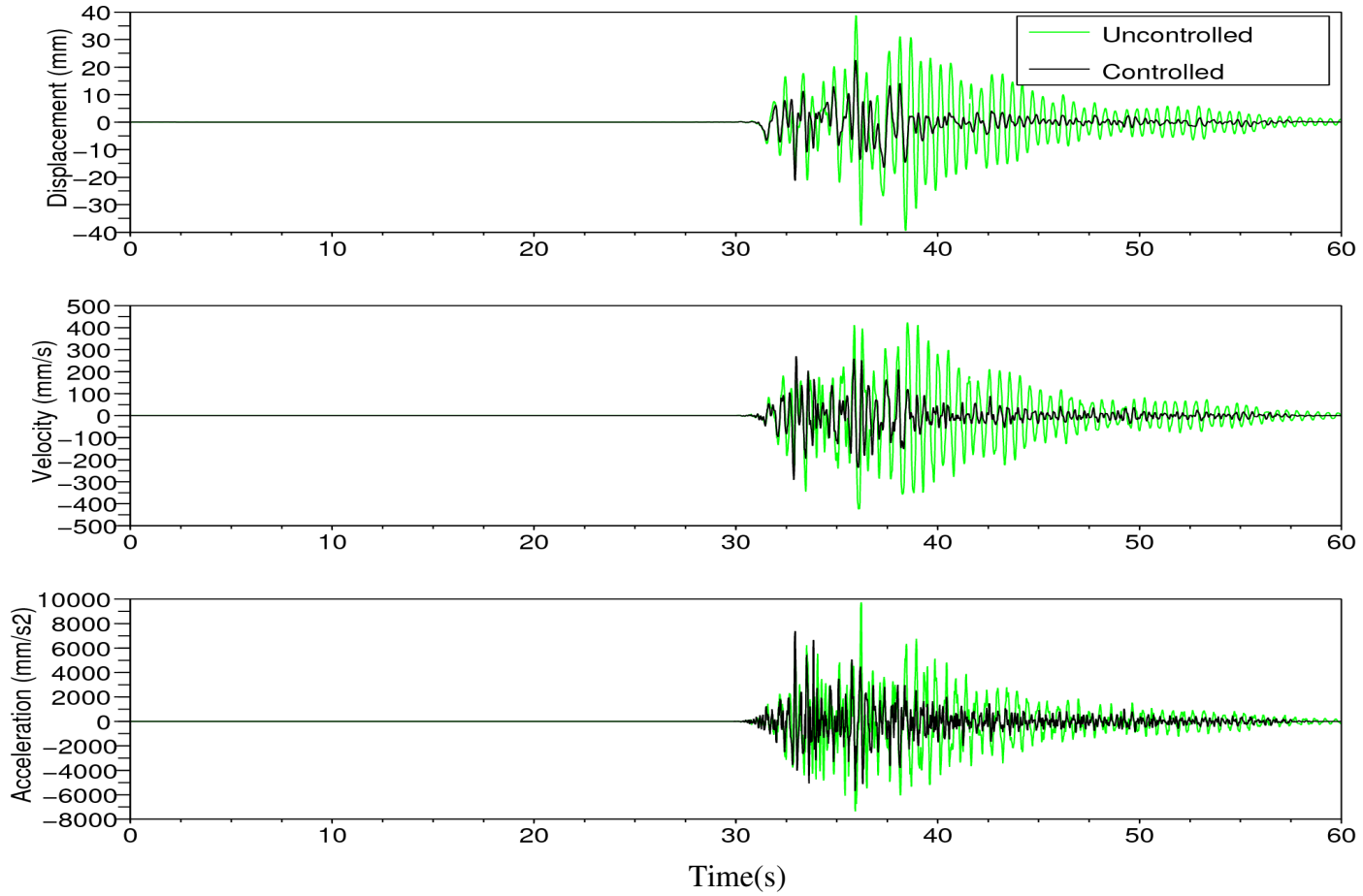

Figure 3.33.Time history of the third floor of the three story structure for Kocaeli-Sakarya earthquake

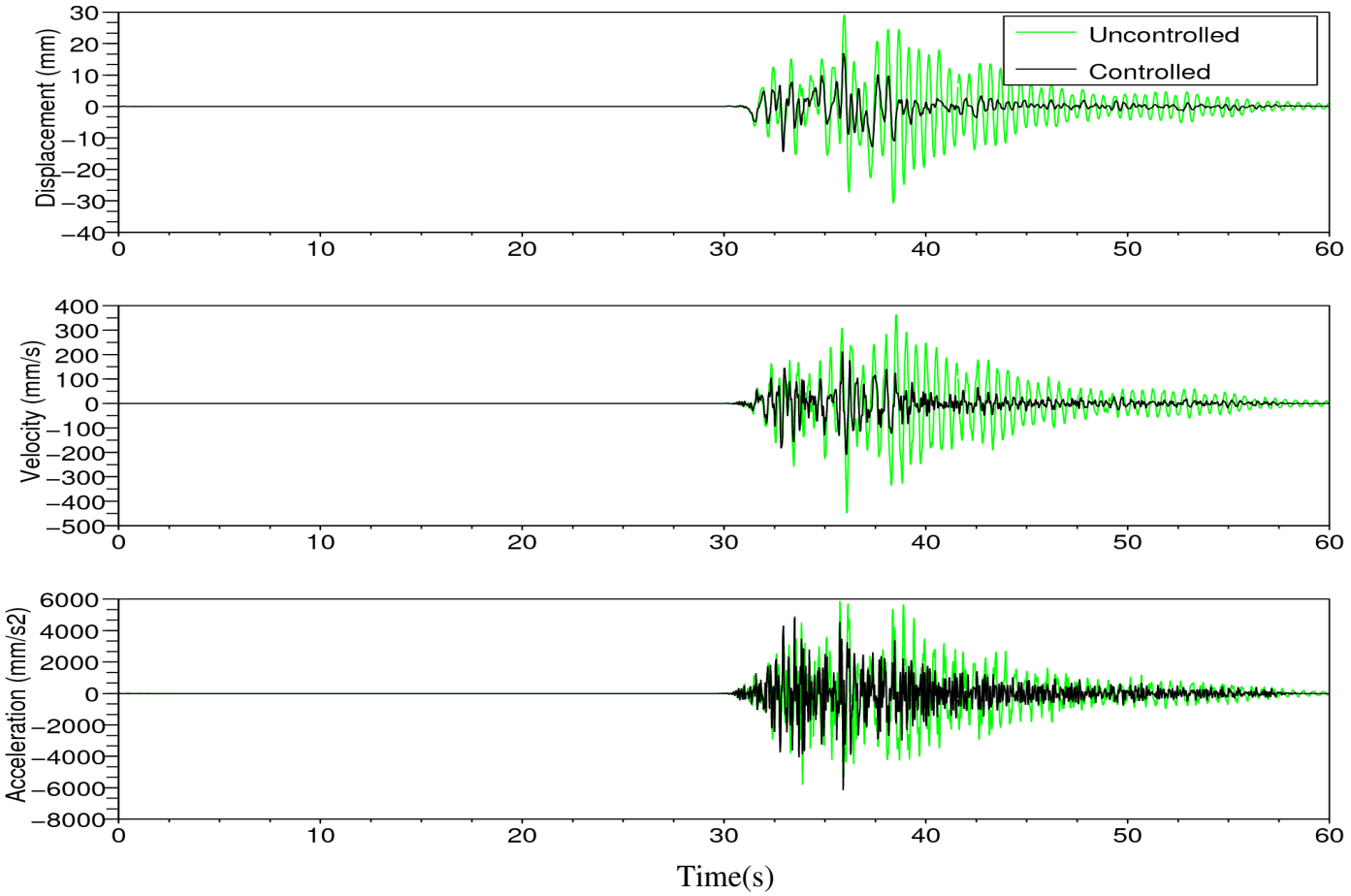

Figure 3.34. Time history of the second floor of the three story structure for Kocaeli-Sakarya earthquake

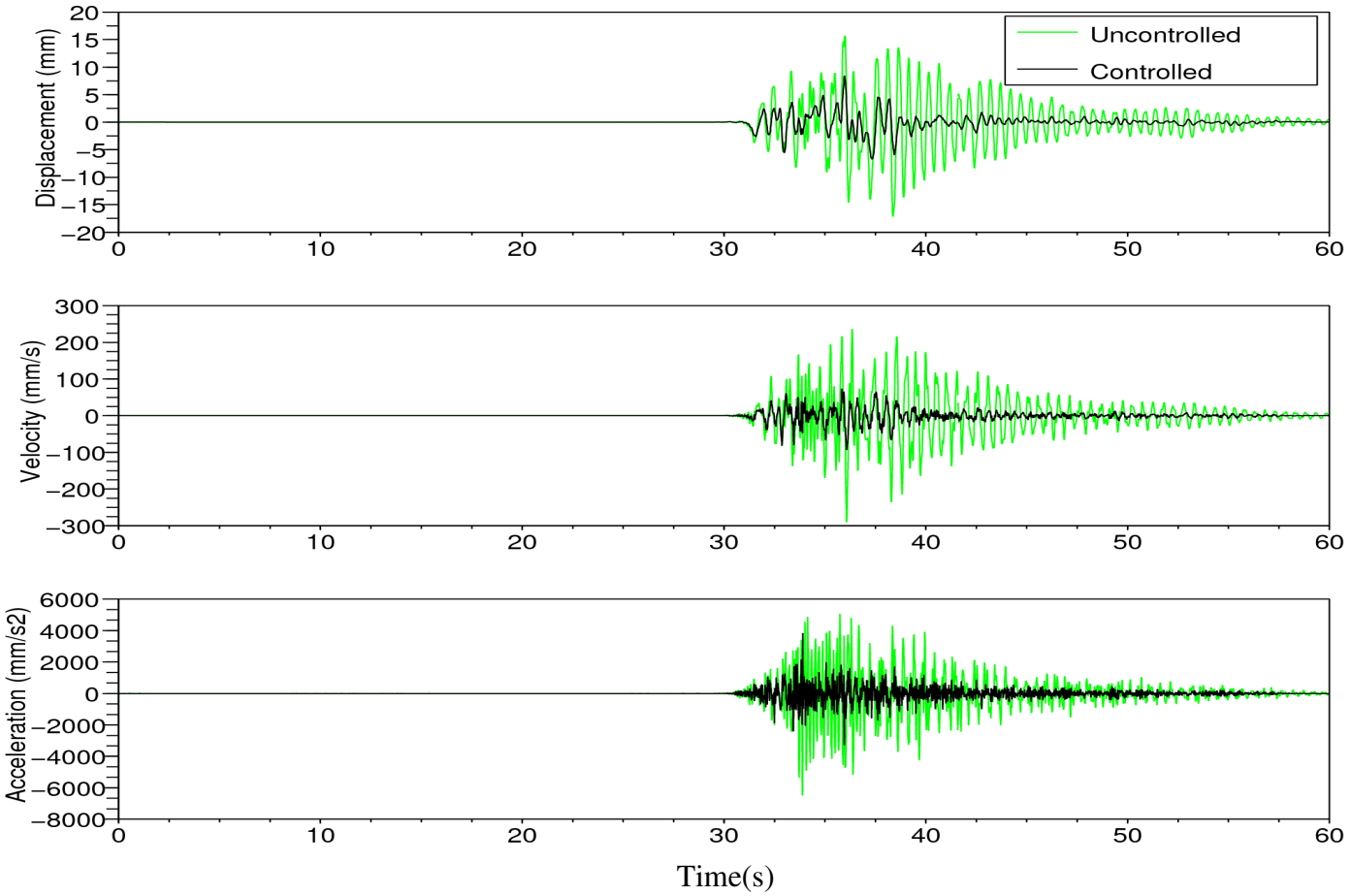

Figure 3.35. Time history of the first floor of the three story structure for Kocaeli-Sakarya earthquake

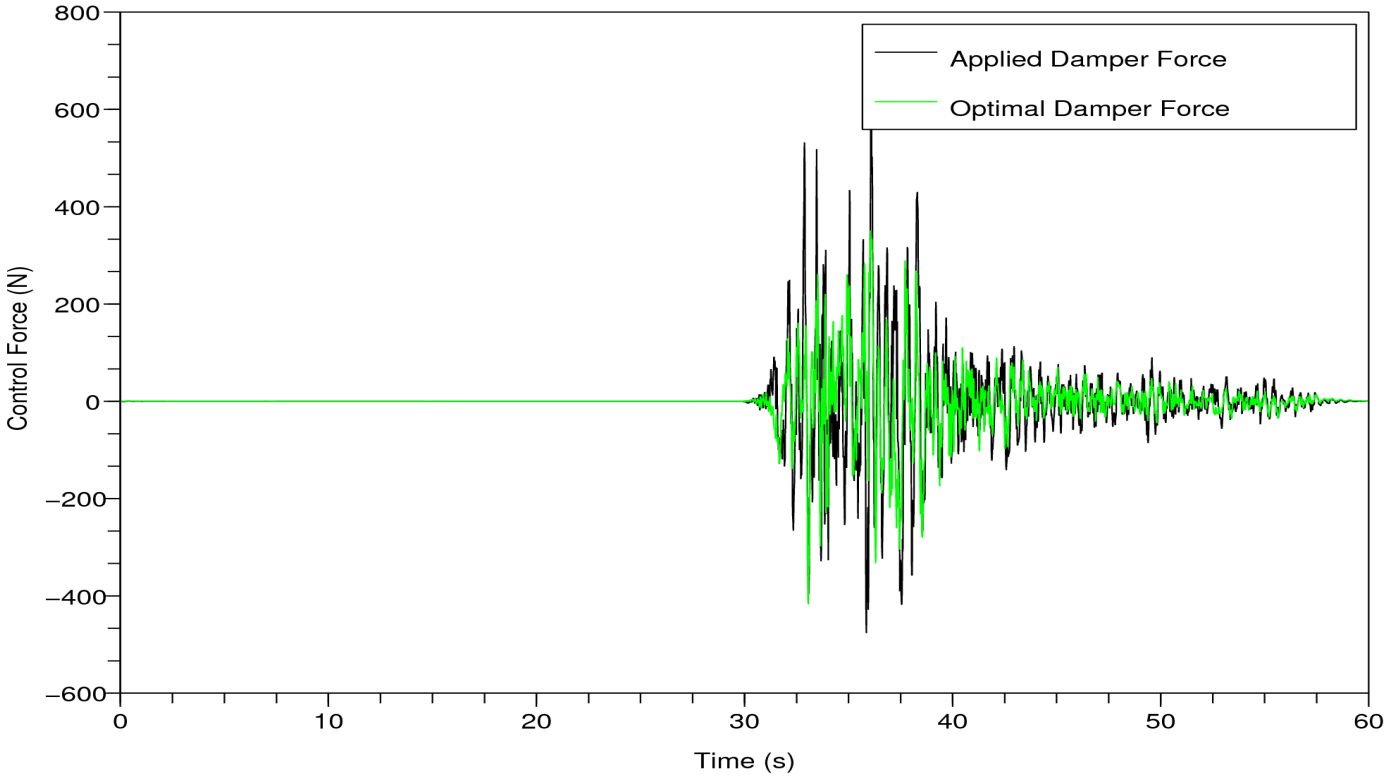

Figure 3.36. Control force evaluated the three story model structure for Kocaeli-Sakarya earthquake

CHAPTER 4

PROPOSED FUTURE WORK

This is a starting step for appliying semi-active control algorthim. Future works in this work may be verified the effect of the proposed control algorithm by using experimental way.

REFERENCES

Chopra, A., 1995. Dynamics of Structures: Theory and Applications to Earthquake Engineering, Second Ed., Prentice Hall, Inc, Upper Saddle River,NJ.

Dyke, S.J., Spencer Jr., B.F., Sain, M.K., and Carlson, J.D. 1998. An Experimental Study of MR Dampers for Seismic Protection, *Smart Materials and Structures: Special Issue on Large Civil Structures*, (7): 693–703.

Rodriguez, M.E., Restrepo J.I. and Blandon J.J. August 2006. Shaking Table Tests of a Four-Story Miniature Steel Building- Model Validation. *Earthquake Spectra*, 22(3):775-780

Sack, R.L., Kuo, C.C., Wu, H.C., Liu, L. and Patten, W.N. 1994. Seismic Motion Control via Semi-active Hydraulic Actuators. *Proceedings of the 5th U.S. National Earthquake Engineering Conference*.

Sadek, F. and Mohraz, B. June 1998. Variable Dampers for Semi-active Control of Flexible Structures. *6th U.S. National Conference in Earthquake Engineering*, Proceedings. Paper No.61 Earthquake Engineering Research Institute,Oakland, CA

Sadek, F. and Mohraz, B. September 1998. Semi-active Control Algorithms for Structures with Variable Dampers. *ASCE Journal of Engineering Mechanics*. 124(9): 981-990.

Symans, M. D. and Constantinou, M.C. 1995. Development and Experimental Study of Semi-Active Fluid Damping Devices for Seismic Protection of Structures. *State Univ. of New York at Buffalo* Report No. NCEER-95-0011.

Symans, M. D. and Constantinou, M.C. January 1997 Seismic Testing of a Building Structure with a Semi-Active Fluid Damper Control System. *Earthquake Engineering and Structral Dynamics*. 26: 759-777.

Yang, J.N., Li, Z. and Vongchavalitkul, S. 1992. A Generalization of Optimal Control Theory: Linear and Nonlinear Structures. *State Univ. of New York at Buffalo* Report No. NCEER-92-0026.

Yang, J.N., Wu, J.C. and Agrawal, A.K. 1995. Sliding Mode Control for Nonlinear and Hysteretic Structures. *ASCE Journal of Engineering Mechanics*. 121(12): 1330-1339.

Yi, F. and Dyke, S.J. June 2000. Structural Control Systems: Performance Assessment. *Proceedings of the American Control Conference Chicago,Illinois*, Vol. 1, 14-18.

Scilab : A free scientific software package, 02/08/2008. http://www.scilab,org/ (accessed August 2, 2008)

PEER Strong Motion Database, 01/07/2008. http://peer.berkeley.edu/smcat/search.html (accessed July 7, 2008)

APPENDIX A

```
//STIFFNESS MATRIX
b=100;//mm
h=10;//mm
I=(b*h^3)/12;//mm4
E=200000;//MPa
L=800;//mm
k=2*12*((E*I)/L^3);//N/mm
K=[k,-k,0;-k,2*k,-k;0,-k,2*k];
//MASS MATRIX
m=(0.100);//N-s2/mm
M=[m,0,0;0,m,0;0,0,m];
//FREKANSLAR
evals=spec(K,M);
w=evals^(1/2);
for m=1:3
  Hz(m)=w(m)/(2*%pi);
end
//PERIODS
for n=1:3
  T(n)=(2*%pi)/w(n);
end
```

```
//MODES

[al,be,Z]=spec(K,M) ;

MQ=Z' * M * Z;

//NORMALIZE MODES

for i=1:3

  for j=1:3

  NQ(j,i)=Z(j,i)/(MQ(i,i)^(1/2));

end

end

//DAMPING MATRIX

c=[2*0.02*w(1),0,0;

   0,2*0.02*w(2),0;

   0,0,2*0.02*w(3)];

C=inv(NQ')*c*inv(NQ);

// sysyem that first three states (x3,x2,x1 ) are displecement of the first,second.third story respectively

// the other states (x6,x5,x4)  are velocity  of the first,second.third story respectively

// x3;third floor displecement,x6;third floor velocity

//u;control signal

//d;disturbance signal

 //*****xdat=A* * x + B1 * d + B2 * u******//

 // **A Matrix**

a1=zeros(3,3);

a2=eye(3,3);

a3=-inv(M)*K;

a4=-inv(M)*C;
```

```
A=[ a1 a2 ; a3 a4];
  //**B1 Matrix**
b1=[0;0;0];
b2=[-1;-1;-1];
B1=[ b1;b2];
  //**B2 Matrix**
b11=[0;0;0];
b22=inv(M)*[0;0;1];
B2=[ b11;b22];
  //******y=C2 * x + D21 * d + D22 * u******//
//**C2 Matrix**
 C2=[eye(6,6); -inv(M)*K -inv(M)*C];
//**D21 Matrix**
D21=[zeros(6,1);b2];   // for absulate displecements and velocities
 //**D22 Matrix**
//D22=zeros(3,1);  //for relative or absulate displecement
D22=[zeros(6,1);b22];  //for absulate displecements and velocities
   //******"z= C1 * x + D11 * d + D12 * u"*****//
R=2;
 C1=[A(4,:)
    A(6,:)
    zeros(1,6)];
D12=[B2(4,:)
     B2(6,:)
          R];
```

```
P12=syslin("c",A,B2,C1,D12);

K_lqr=lqr(P12);

K_lqr=real(K_lqr);

sp2=spec(A+B2*K_lqr);

//***********LQE*************

nx=size(A,1);

ne=size(B2,2);

ny=size(C2,1);

G=B2;

Q_e(ne,ne)=.1; R_e=10*eye(ny,ny); N=zeros(ne,ny);

bigR =[G*Q_e*G' G*N;N'*G' R_e];

[W,Wt]=fullrf(bigR);B_e=W(1:size(G,1),:);

D_e=W(($+1-size(C2,1)):$,:);

C_e=C2;

P_e=syslin('c',A,B_e,C_e,D_e);

[K_e,X_e]=lqe(P_e);

//Riccati check:

S=G*N;Q=B_e*B_e';

norm((A-S*inv(R_e)*C_e)*X_e+X_e*(A-S*inv(R_e)*C_e)'-
X_e*C_e'*inv(R_e)*C_e*X_e+Q-S*inv(R_e)*S');

//Stability check:

spec(A+K_e*C_e);

//Disturbance in El-Centro

getf('/home/hakan/Desktop/scilab_thesis/earthquake_records/okuma_prg/oku_eq.sci');

[X,t]=oku_eq('/home/hakan/Desktop/scilab_thesis/earthquake_records/el_centro/I-
ELC180_AT22.txt');
```

```
d=9810*X;//d:mm/s^2
tf=15;  // saniye
dt=t(2)-t(1);
t=t(1):dt:tf;
nt=length(t);
d=d(1:nt);
/CLOSED LOOP SIMULATION
//A_cl Matrix
A_cl=[A+B2*K_lqr];
//C_cl Matrix
C_cl=[C2+D22*K_lqr];
//xo=zeros(6,1);
xo=0*ones(6,1);
[sys_cl]=syslin('c',A_cl,B1,C_cl ,D21,xo);
sys_ol=syslin('c',A,B1,C2 ,D21,xo);
[y_cl, x_cl]=csim(d,t,sys_cl);
[y_ol, x_ol]=csim(d,t,sys_ol);
scf; plot2d(t,y_ol(1,:),3)
    plot2d(t,y_cl(1,:),1)
scf; plot2d(t,y_ol(7,:),3)
    plot2d(t,y_cl(7,:),1)
//********Kalman Filter******************
A_1=[A];
A_2=[B2*K_lqr];
A_3=(-K_e*C2);
```

```
A_4=[A+K_e*C2+B2*K_lqr];

A_obs=[A_1 A_2;A_3 A_4];

B_obs=[B1;B1];

C_obs=eye(12,12);

s_obs=syslin('c',A_obs,B_obs,C_obs);

//x0_obs=[zeros(6,1);zeros(6,1)];

x0_obs=[0*ones(6,1);zeros(6,1)];

[y_e,x_e] = csim(d,t,s_obs,x0_obs);

//Estimated states x4,x5,x6

scf();plot2d(t,y_e(4,:),1),plot2d(t,x_e(10,:),2),legend('Original state , x4', 'estimated state , x4_e');xgrid(1);

scf();plot2d(t,x_e(5,:),1),plot2d(t,x_e(11,:),2),legend('Original state , x5', 'estimated state , x5_e');xgrid(1);

scf();plot2d(t,x_e(6,:),1),plot2d(t,x_e(12,:),2),legend('Original state , x6', 'estimated state , x6_e');xgrid(1);
```